UNIVERSIDADE FEDERAL DO CEARÁ

CENTRO DE TECNOLOGIA

DEPARTAMENTO DE ENGENHARIA METALURGICA E DE MATERIAIS

PROGRAMA DE PÓS-GRADUAÇÃO EM ENGENHARIA E CIÊNCIA DE MATERIAIS

JEAN JEFFERSON MORAES DA SILVA

AN ATOMIC REDISTRIBUTION STUDY OF THE PHASE TRANSFORMATION KINETICS OF MARAGING-300 STEEL

FORTALEZA

2018

JEAN JEFFERSON MORAES DA SILVA

AN ATOMIC REDISTRIBUTION STUDY OF THE PHASE TRANSFORMATION KINETICS OF MARAGING-300 STEEL

Tese apresentada ao Programa de Pós-Graduação em Engenharia e Ciência de Materiais da Universidade Federal do Ceará, como requisito parcial à obtenção do título de Doutor em Engenharia e Ciência de Materiais. Área de concentração: Propriedades Físicas e Mecânicas dos Materiais.

Orientador: Prof. Dr. Hamilton Ferreira Gomes de Abreu.
Coorientador: Prof. Dr. Igor Frota de Vasconcelos.

FORTALEZA
2018

Dados Internacionais de Catalogação na Publicação
Universidade Federal do Ceará
Biblioteca Universitária
Gerada automaticamente pelo módulo Catalog, mediante os dados fornecidos pelo(a) autor(a)

S58a Silva, Jean Jefferson Moraes da.
An atomic redistribution study of the phase transformation kinetics of Maraging-300 Steel / Jean Jefferson Moraes da Silva. – 2018.
91 f. : il. color.

Tese (doutorado) – Universidade Federal do Ceará, Centro de Tecnologia, Programa de Pós-Graduação em Engenharia e Ciência de Materiais, Fortaleza, 2018.
Orientação: Prof. Dr. Hamilton Ferreira Gomes de Abreu.
Coorientação: Prof. Dr. Igor Frota de Vasconcelos.

1. Maraging-300. 2. Espectroscopia Mössbauer. 3. Composto intermetálico. 4. Difração de raios-X. 5. Microscopia eletrônica de transmissão. I. Título.

CDD 620.11

JEAN JEFFERSON MORAES DA SILVA

AN ATOMIC REDISTRIBUTION STUDY OF THE PHASE TRANSFORMATION KINETICS OF MARAGING 300 STEEL

Thesis presented to the Post-Graduate Program in Materials Science and Engineering of the Federal University of Ceará, as a partial requisite to obtain a Doctor degree in Materials Science and Engineering. Concentration area: Physical and Mechanical Properties of Materials.

Approved at: 21 /08 /2018.

THESIS COMMITTEE

_____

Prof. Dr. Hamilton Ferreira Gomes de Abreu (Advisor)

Universidade Federal do Ceará (UFC)

_____

Prof. Dr. Igor Frota de Vasconcelos (Co-advisor)

Universidade Federal do Ceará (UFC)

_____

Prof. Dr. José Marcos Sasaki

Universidade Federal do Ceará (UFC)

_____

Prof. Dr. Carlos Augusto Silva de Oliveira

Universidade Federal de Santa Catarina (UFSC)

_____

Prof. Dr. Andrea Paesano Júnior

Universidade Estadual de Maringá (UEM)

To my wife Cintia for her unconditional affection and communion.

To my family and to my father (in memoriam).

ACKNOWLEDGEMENT

To all the members of my family, especially to my wife Cintia, my parents João (in memoriam) and Lêda, my sister Sarah and my brother Renan and to our pet who daily contribute in my development as a human being.

To my eternal mentor Professor Dr. Hamilton Ferreira Gomes de Abreu for being my advisor and for all the support granted since graduation times and for becoming one of my references either in personal and professional aspects.

To Professor Dr. Igor Frota de Vasconcelos for becoming my co-advisor throughout the construction of this thesis and also for the trust in granting me free access to his laboratory.

To Professor Dr. Carlos Augusto Silva de Oliveira and to Dr. Pedro Henrique Lamarão Souza for the great support in the accomplishment and interpretation of analyzes in Transmission Electron Microscopy in the UFSC.

To the fellows of the Advanced Materials Laboratory Msc. Francisco Iran Sousa da Silva, Dr. Thiago Soares Ribeiro, Msc. Kleyton Jânio Camelo and Msc. Francisco Gilvane Sampaio de Oliveira for the great help in the experiments of Mössbauer spectroscopy as well as in the accomplishment of some heat treatments.

To the colleagues Professor Dr. Mohammad Masoumi and Msc. Luis Paulo Mourão dos Santos for the companionship and technical teachings provided throughout the thesis.

To Professor Dr. José Marcos Sasaki and Msc. Diego Felix Dias for the elucidations regarding X-ray diffraction, as well as some experiments in his laboratory.

To all the undergraduate students of Lacam who at some moment supported me in the experimental procedures of this thesis.

To Professor Dr. Cleiton Carvalho Silva and Msc. Émerson Mendonça Miná for the support in some SEM analyzes and thermochemical calculations.

To Professor Dr. Elineudo Pinho de Moura for the help in the development of the algorithms in the quantification work still in development.

To Professor Dr. Marcelo José Gomes da Silva for the elucidations about TEM.

To the laboratory colleagues Flávio, João, Waydson, Venceslau, Natan, Isabel, Juliane, Pablo, Regina, Tathiane, Jorge, Oliveira e Mauro who contributed a lot in the exchanges of ideas as well as for the pleasant research environment.

To the IFCE (Pecém campus) directors and to the teachers of the mechanical area of this campus for the release of my activities at the final stage, fundamental for the conclusion of this thesis.

Last but not least, to God for providing me with this experience of life and ensuring the health and harmonious coexistence of all the people mentioned above.

RESUMO

Os aços maraging são uma classe de aços com base em Fe que são envelhecidos pela precipitação de compostos intermetálicos finamente dispersos em uma matriz martensítica de baixo carbono. A combinação de propriedades mecânicas e magnéticas apropriadas torna-o um material adequado para aplicações estratégicas nas indústrias aeronáutica, aeroespacial e nuclear. Os principais elementos de liga neste aço são Ni, Co, Mo e Ti. O carbono é considerado uma impureza, e o alto teor de níquel (18% wt.) garante que a martensita (α′) se forme no resfriamento a ar. O processamento térmico dos aços maraging envolve um tratamento de solubilização, geralmente a 820°C por 1 h, para dissolver homogeneamente os elementos de liga na matriz austenítica nesta temperatura. A matriz martensítica de baixo carbono formada é então endurecida pela precipitação em fina escala de compostos intermetálicos a temperaturas entre 400-650°C (processo de envelhecimento), induzida pela redistribuição de átomos. Precipitados como as fases Ni_3 (Ti, Mo)-η, Fe_2Mo-Laves, fase S, ω e fase Fe_7Mo_6-μ foram relatados e a reversão para austenita (γ) também foi observada em temperaturas mais altas e tempos de envelhecimento mais longos. Nos aços maraging, os precipitados conhecidos apresentam escala nanométrica com dimensões entre 1 e 50 nm. Além disso, a baixa fração volumétrica dessas fases dificulta sua análise. Por causa disso, muitas incertezas ainda existem em relação à cinética de precipitação neste material e não há curvas de tempo-temperatura-transformação (TTT) para este tipo de aço maraging na literatura. Devido ao alto teor de Fe do aço Maraging-300, a espectroscopia Mössbauer de transmissão (EMT) foi escolhida como uma técnica capaz de fornecer informações valiosas sobre a mobilidade atômica neste material. Nesta tese, o aço Maraging-300 foi submetido a processamento térmico resultando em 25 diferentes condições de envelhecimento. Espectroscopia Mössbauer de transmissão (EMT) - com o auxílio de microscopia eletrônica de transmissão (MET), difração de raios-X (DRX), microscopia ótica e medidas de dureza Vickers - foi utilizada para investigar o efeito da mobilidade e configuração dos átomos de impureza na transformação de fases e no comportamento de precipitação do aço. Foram estudadas temperaturas entre 440 e 600°C e tempos de 1 a 100 h de envelhecimento. Os principais resultados deste trabalho revelaram que a precipitação de compostos intermetálicos em

uma matriz martensítica rica em Co ocorre na maioria das condições estudadas. A redistribuição atômica é intensa nas primeiras horas de envelhecimento e Ni, Mo e Ti são os principais elementos que formam precipitados. Fases metastáveis aparecem em baixas temperaturas de envelhecimento e austenita reversa foi evidenciada em temperaturas mais altas e tempos de envelhecimento mais longos. Em temperaturas de envelhecimento mais altas (≥ 520°C), o teor de Fe da matriz martensítica diminui com o tempo de envelhecimento, e assim que a austenita começa a se formar, a redistribuição atômica ocorre principalmente entre esta fase e os precipitados. Também nestas últimas condições, uma zona de transição cristalina / magnética foi detectada no material.

Palavras-chave: Maraging-300. Espectroscopia Mössbauer. Composto intermetálico. Difração de raios-X. Microscopia eletrônica de transmissão.

ABSTRACT

Maraging steels are a class of Fe-based alloying steels that are age-hardened by the precipitation of finely dispersed intermetallic compounds in a low-carbon martensitic matrix. The combination of appropriate mechanical and magnetic properties makes it a suitable material for strategic applications in the aeronautical, aerospace and nuclear industries. The main alloying elements in this steel are Ni, Co, Mo and Ti. Carbon is considered an impurity, and the high nickel content (18 wt% Ni) ensures that martensite (α′) forms on air cooling. Thermal processing of maraging steels involves a solution treatment, usually at 820°C for 1 h, to homogeneously dissolve the alloying elements at the austenitic matrix at this temperature. The formed low carbon bcc martensitic matrix is then hardened by fine-scale precipitation of intermetallic compounds at temperatures of 400–650°C (ageing process), induced by the redistribution of atoms. Precipitates like the Ni_3(Ti,Mo) η-phase, Fe_2Mo Laves phase, S phase, ω phase, and Fe_7Mo_6 μ-phase were reported and reversion to austenite (γ) was also noticed at higher temperatures and longer ageing times. In maraging steels, the known precipitates present nanometric scale with dimensions between 1 and 50 nm. Besides this, the low volume fraction of such phases makes them hard to analyse. Because of this, too many uncertainties still exist regarding the precipitation kinetics in this material and there are no time-temperature-transformation (TTT) curves for this grade of maraging steel on literature. Because of the high Fe content of Maraging-300 steel, transmission Mössbauer spectroscopy (TMS) was chosen as a technique capable of providing valuable information about atomic mobility in this material. In this thesis, Maraging-300 steel was subjected to thermal processing resulting in 25 different ageing conditions. Transmission Mössbauer spectroscopy (TMS) – with the aid of transmission electron microscopy (TEM), X-ray diffraction (XRD), optical microscopy, and Vickers hardness measurements – has been used to investigate the effect of the mobility and configuration of the non-iron atoms on the phase transformation and precipitation behaviour of the steel. Ageing temperatures from 440 to 600°C for times from 1 to 100 h of ageing were studied. The key findings of this work revealed that the precipitation of intermetallic compounds in a bcc Co-rich martensitic matrix occurs in most of the conditions studied. The atomic

redistribution is intense in the first hours of ageing and Ni, Mo and Ti are the main elements that form precipitates. Metastable phases appear at low ageing temperatures and reverted austenite was evidenced at higher temperatures and longer ageing times. At higher ageing temperatures (≥ 520°C) the Fe content of the martensitic matrix decreases with ageing time, and as soon as austenite begins to form much of the atomic redistribution occurs mainly between this phase and the precipitates. Also at these latter conditions a crystalline/magnetic transition zone was detected in the material.

Keywords: Maraging-300. Mössbauer spectroscopy. Intermetallic compound. X-ray diffraction. Transmission electron microscopy.

LIST OF FIGURES

LIST OF TABLES

LIST OF ACRONYMS

BCC	Body Centred Cubic
FCC	Face Centred Cubic
RT	Room Temperature
SADP	Selected Area Diffraction Pattern
SANS	Small-Angle Neutron Scattering
SAXS	Small-Angle X-ray Scattering
ST	Solution-treated
TEM	Transmission Electron Microscopy
TMS	Transmission Mössbauer Spectroscopy
TTT	Time-Temperature-Transformation
XRPD	X-ray Powder Diffraction

LIST OF SYMBOLS

α′	Martensite
η	Hexagonal/Orthorhombic A_3B phase
S	Hexagonal A_8B phase
ω	Hexagonal A_2B phase
μ	Rhombohedral A_7B_6 phase
γ	Austenite
Kα	Characteristic radiation
λ	Wavelength
α-Fe	Ferrite
B_{hf}	Magnetic Hyperfine Field
Fe^0	Zero Valence iron
δ	Isomer Shift
2ε	Quadrupole Splitting
^{57}Fe	Mössbauer isotope
σ	Tetragonal AB phase
X	Hexagonal A_3B phase
a_{hkl}	Lattice constant

SUMMARY

1 INTRODUCTION

This chapter briefly introduces the maraging steels, the objective of this thesis and some initial remarks.

1.1 Literature Overview

It was the year of 1958 when two researchers (R.F. Decker and C. Bieber) decided to join their expertise in precipitation-hardened super alloys to create something bearing the large increment of improvement over the metallurgical state-of-art of that year. Originally their primary target was the development of a material suitable for submarine hulls. But the space race of the 1960's was very much alive and the development of maraging steels was quite convenient for the aerospace industry's goals. In addition, a large amount of industrial applications for this material began to emerge and this increased the demand for its development.

In the first years of development of the material, a series of studies were carried out in order to investigate the material and to know its behaviour on subjects such as welding, corrosion, machining, etc. In addition to investigating about their physical metallurgy, role of alloying elements, types of heat treatment used, etc. These studies were compiled and can be found in the references at the end of this chapter [1,2]. Other literature reviews about the material and the main techniques used in this work can also be found at the introduction and the end of each chapter.

The term "Maraging" was adopted as the generic term for the alloy system of ageing of the martensitic matrix. The austenite-martensite transformation in iron-nickel alloys was studied by Jones and Pumphrey [3] and the transformation characteristics are illustrated in figure 1.1

Figure 1.1 – Fe-Ni transformation diagram.

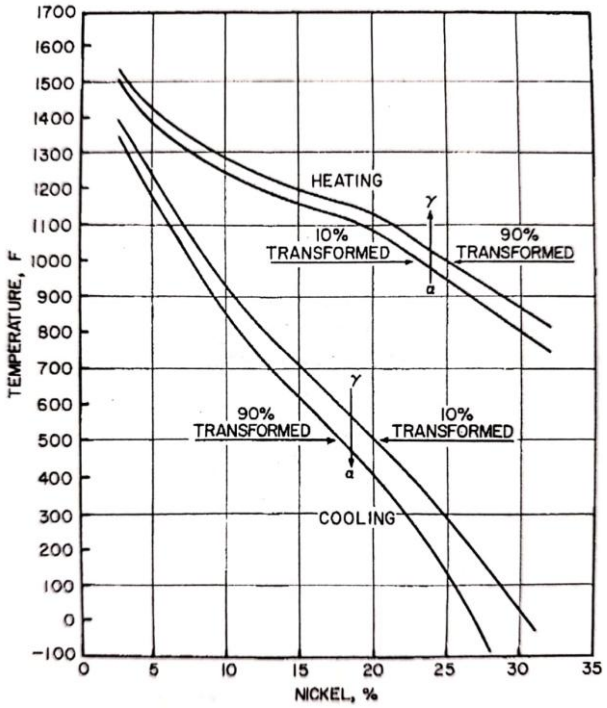

Source: Jones and Pumphrey [3]

The martensitic phase formed at maraging steels presents different characteristics when compared to that of conventional carbon steels. The rapid quenching is not required and the martensite is moderately hard. The transformation can proceed both isothermally and athermally. The martensite presents a body-centered cubic structure or at most shows a minimal distortion, rather than the tetragonal structure commonly presented. Finally, the hysteresis of the transformation seen in figure 1.1 allows considerable reheating of martensite for ageing before reversion to austenite occurs [2].

At first the amount of Ni at these steels was between 20 and 25%. However these grades were soon abandoned on account of their brittleness at ultra-high-strength levels [4]. The early experiments discovered a remarkable synergistic effect from cobalt and molybdenum. Because of this, the main alloying elements are Ni (usually around 18% wt.), Co and Mo. Some Ti and Al, among other chemical elements, are also added most often to get the best properties of the steel. The Fe-18%Ni composition was chosen as the alloy base since higher nickel contents led to retained austenite. [1] Table 1.1 shows the main types of maraging steels and their respective nominal compositions and years of release.

Table 1.1 – Nominal compositions of Ni-Co-Mo maraging steels (wt%.)

Alloy	Ni	Co	Mo	Ti	Al	Year announced
18Ni(200)	17-19	8-9	3-3.5	0.15-0.25	0.05-0.15	1960
18Ni(250)	17-19	7-8.5	4.6-5.2	0.3-0.5	0.05-0.15	1960
18Ni(300)	18-19	8.5-9.5	4.6-5.2	0.5-0.8	0.05-0.15	1960
18Ni(350)	17.5-18.5	12-12.5	3.8-4.6	1.4-1.7	0.10-0.15	1968
13Ni(400)	13	15-16	10	0.2	-	1968

Source: Adapted from Magnée et al. [1]

Maraging steels are characterized by their very low carbon content and the use of substitutional elements to produce age-hardening in Fe-Ni martensite [1]. The heat-treatment of maraging steels consists in solution annealing for 1 h at 815°C. Although other annealing temperatures or multiple annealing treatments are used in certain cases [1]. The aim of the solution treatment is to homogeneously dissolve the alloying elements in the martensitic matrix. In the as-annealed condition, the alloys have a hardness of the order of 30 HRc and can be readily machined or fabricated [1]. The hardening is then achieved by the precipitation of intermetallic compounds generally for 3 h at 480°C. Other ageing times and temperatures are also used for specific purposes. The hardening effect comes up by the formation of finely distributed precipitates that present an effective barrier to the motion of dislocations. The strengthening is related to the stress required for dislocations to cut through or pass by precipitates. Some care should be taken regarding the ageing time of the material, avoiding that the precipitates grow too much which will cause the overaging phenomena. Depending on the temperature, the reversion to the austenitic phase can also occurs.The main phases that occur in maraging steels were listed by Tewari [5] and are shown in table 1.2.

Table 1.2 – Phases observed in maraging steel.

Phase	Stoichiometry	Crystal structure	Lattice parameters	Orientation relationship
γ		f.c.c.	$a = 3.5852\,^{\circ}A$	
α		b.c.c.	$a = 2.8812\,^{\circ}A$	$\{110\}_{b.c.c.}//\{111\}_{f.c.c.}$ $\langle 111\rangle_{b.c.c.}//\langle 110\rangle_{f.c.c.}$
μ	A_7B_6	rhombohedral	$a = 4.751\,^{\circ}A$ $\alpha = 30.38^{\circ}$	
ω	A_2B	hexagonal	$a = 3.9–4.05\,^{\circ}A$ $c = 2.39–2.48\,^{\circ}A$	
S	A_8B	hexagonal	$a = 7.04\,^{\circ}A$ $c = 2.48\,^{\circ}A$	
X	A_3B	hexagonal	$a = 2.55\,^{\circ}A$ $c = 8.30\,^{\circ}A$	$(0001)_X//\{111\}_\alpha$ $\langle \bar{2}110\rangle_X//\langle 110\rangle_\alpha$
Fe_2Mo	A_2B	hexagonal	$a = 4.745\,^{\circ}A$ $c = 7.754\,^{\circ}A$	$(0001)_{Fe_2Mo}//\{110\}_\alpha$ $\langle \bar{2}110\rangle_{Fe_2Mo}//\langle 110\rangle_\alpha$
$Ni_3(Ti, Mo)$	A_3B	hexagonal	$a = 5.101\,^{\circ}A$ $c = 8.307\,^{\circ}A$	$(0001)_{Ni_3Ti}//\{001\}_\alpha$ $\langle 11\bar{2}0\rangle_{Ni_3Ti}//\langle 111\rangle_\alpha$
Ni_3Mo	A_3B	orthohombic	$a = 5.064\,^{\circ}A$ $b = 4.224\,^{\circ}A$ $c = 4.448\,^{\circ}A$	

Source: Tewari et al. [5]

The study of the phase transformation kinetics of the maraging steels is of extreme importance for the knowledge of the most varied conditions of use of the material, making it possible to suggest some variation of composition in the material in order to obtain even better properties related to its use. In addition, a better understanding of their precipitation kinetics allows us to suggest more adequate heat treatments, using the material as efficiently as possible.

1.2. Motivation for the thesis

Despite the amount of research that has been carried out since the first years of study of the material until the present time, there are still many uncertainties regarding the phase transformation process of maraging steels. The size of the precipitates as well as their volumetric fraction makes the material hard to analyse by conventional techniques and at this time there are still no TTT diagrams for all types of maraging steel. In fact, the only existing TTT diagram is that suggested by Tewari et al. [5] for Maraging-350 steel. Thus, many doubts still exist regarding the phase precipitation kinetics of this type of material, as well as some uncertainties about the existence or not of precipitates and which types of precipitates occur at certain ageing conditions. This thesis is focused on an innovative approach, based mainly on Mössbauer spectroscopy, to better understand the phase transformation process and the ageing kinetics of Maraging-300 steel through the atomic redistribution of the material.

1.3. Objectives of the thesis

- Investigate the effects of low and high ageing temperature heat-treatments on phase transformation process of Maraging-300 steel.
- Find a correlation between the atomic redistribution, precipitation behaviour and the improvement of mechanical properties at the material.
- Perform a qualitative analysis of the phase transformation and precipitation behaviour of the material.

1.4. Thesis organization

To fulfil the above-mentioned objectives, this thesis has been organized in chapters based on a transcription of papers that will be published covering all the ageing conditions of interest in the material.

In the second chapter an experimental procedure including all conditions studied is shown. In the third chapter the conditions in the most usual ageing temperature were analysed. In the fourth chapter the low ageing temperature conditions were studied. The fifth chapter investigates the high ageing temperature conditions. All these chapters performed a qualitative analysis through the techniques cited in their experimental procedures.

Finally at chapter 6 some concluding remarks are shown and an innovative study involving Mössbauer spectroscopy is suggested as a future work, at this time in a more quantitative approach in all the ageing conditions studied in this thesis.

REFERENCES

[1] A. Magnée, J.M. Drapier, J. Dumont, D. Coutsouradis, L. Habraken, Cobalt-containing High-strength Steels, Centre d'Information du Cobalt, Brussels, 1974.

[2] R.F. Decker, Notes on the development of Maraging steels, in: Source book of Maraging steels, American society for Metals, Ohio, 1979.

[3] F.W. Jones and W.I. Pumphrey, Free energy and metastable states in the iron-nickel and iron-manganese systems, Journal, Iron and Steel Institute, Vol. 163, 1949, p. 121.

[4] A.M. Hall, Review of maraging steel developments, Cobalt, No. 24, 138, 1964.

[5] R. Tewari, S. Mazumder, I.S. Batra, G.K. Dey, S. Banerjee, Precipitation in 18 wt% Ni Maraging steel of grade 350, Acta Mater. 48 (2000) pp. 1187–1200.

2 EXPERIMENTAL PROCEDURE

Maraging steel of grade 300 (see composition in Table 2.1) was obtained as a forged billet in solution-treated condition (825°C for 10 h, oil cooled) as informed by the manufacturer. The material was cut into small pieces of about 15 × 12 × 2 mm, austenitised at 820°C for 30 min, and then water cooled to room temperature (RT) to form martensite. Samples were then aged at 440, 480, 520, 560 and 600°C for periods of 1, 3, 10, 50, and 100 h, and then water cooled.

Table 2.1 -.Chemical composition of Maraging-300 steel.

	Ni	Co	Mo	Ti	Al	Mn	Si	Cr	Cu	V	C	Fe
wt%	18.33	9.41	4.99	0.78	0.10	0.01	0.04	0.11	0.02	0.02	0.007	Bal.

Source: Own author.

For each ageing condition, the same sample was used for each of the analytical techniques. Each sample was grinded to half thickness, then immersed for 30 s in a solution of 5% hydrofluoric acid in hydrogen peroxide to eliminate the surface layer, thus eliminating any possible phase transformation (γ→α′) caused by mechanical grinding, as reported by Pardal et al. [6]. This solution was used as the final step of sample preparation for XRPD and TMS measurements.

X-ray powder diffraction patterns were measured at RT using Co-Kα radiation (λ = 1.78901 Å) with 40 kV and 45 mA. All measurements were carried out using a PANalytical® diffractometer, model X'Pert Pro, with a step size of 0.02°, counting time of 2 s, and an angular interval of 45–130° with monochromator. A divergent slit of 2° and a receiving slit of 1.5 mm were used at the measurement. The PANalytical® software X'Pert HighScore was used for data treatment.

The same samples as used for XRPD were then mounted and polished for Vickers hardness measurements, carried out in a Shimadzu TH710 tester using a 1 kg load and 15 s indentation time. An internal average of 4 from 6 impressions was made for each condition.

For optical microscopy, with the aim of revealing the small fraction of reverted austenite in the sample aged at 480°C for 100 h, a modified Fry reagent consisting of 150 ml water, 50 ml hydrochloric acid, 25 ml nitric acid, and 1 g copper chloride was used at RT. A Zeiss Axiocam ICc 5 microscope was used for optical analysis.

Some samples were prepared for TEM analysis by grinding to a thickness of about 0.12 mm. 3 mm disc-shaped thin foil specimens were electropolished using Struers® equipment, model TenuPol-5. The electrolytic solution consisted of 6% perchloric acid in acetic acid, at −3°C and 21 V. TEM analyses were carried out in a JEOL® JEM-1011 transmission electron microscope with 100 kV of accelerating voltage.

For TMS measurements, all the thin samples were grinded to a thickness of about 0.06 mm. After grinding, the previously described acid solution was used with the same aim, in addition to further reducing the thickness of the material. Spectra were taken at RT from a constant acceleration spectrometer with a ^{57}Co(Rh) source. The largest Doppler velocity was 8 mm/s. The equipment was calibrated with metallic iron (α-Fe) at RT.

3 AN ATOMIC REARRANGEMENT INVESTIGATION OF THE 480°C PHASE TRANSFORMATION PROCESS IN MARAGING-300 STEEL

3.1 Review

Maraging steels are known to achieve the best mechanical properties when aged around 480°C. However, the precipitate formation process is still not clear enough at this temperature. In this paper Mössbauer spectroscopy– with the aid of transmission electron microscopy, X-ray diffraction, hardness measurements, and optical microscopy - were used to investigate the phase transformation process of solution-treated and 480°C-aged Maraging-300 steel specimens. The results indicated that the precipitation of intermetallic compounds, which are responsible for the improvement of mechanical properties starts at the early stages of ageing, but without iron atoms on its stoichiometry. Atomic mobility is discussed and precipitate formation is evidenced. Small amounts of reverted austenite as a consequence of precipitate dissolution were detected at longer ageing times, and the formation of paramagnetic iron-rich phases is suggested as well.

3.2 Introduction

Maraging steels are a class of alloying steels used mainly for structural applications that require ultra-high strength and high fracture toughness. Due to this, maraging steels are indicated for strategic applications in the aerospace, aeronautical, and nuclear industries.

The main alloying elements of this kind of steel are Ni, Co, Mo, and Ti. Maraging steels are divided into sub-classes – 200, 250, 300, 350, and 400 – according to their yield strength (ksi) [1]. Despite the low carbon content (carbon is considered an impurity), the high nickel content (18 wt% Ni) of the maraging steels ensures that martensite (α′) forms on air cooling [2]. The low carbon bcc martensitic matrix is then hardened by fine-scale precipitation of intermetallic compounds, such as the $Ni_3(Ti,Mo)$ (η-phase). Other phases, like the Fe_2Mo (Laves phase), S phase, ω phase, and Fe_7Mo_6(μ-phase) were also reported in early studies on 300 and 350 grade maraging steels aged at 400–600°C [3,4]. Reversion to austenite (γ) was also noticed at higher temperatures and longer ageing times [5–7].

Thermal processing of maraging steels involves a solution treatment, usually at 820°C for 1 h, to homogeneously dissolve the alloying elements at the iron austenite matrix [8,9]. The so-called ageing process comes subsequently, at temperatures of 400–650°C, inducing redistribution of atoms and consequently the formation of the intermetallic compounds.

Because of the nanometric structure of such phases, a variety of techniques have been used to study their precipitation behaviour: transmission electron microscopy (TEM) [5], small angle X-ray scattering (SAXS) [10], small angle neutron scattering (SANS) [11], electrolyte extraction method [12], positron annihilation [13], and Mössbauer spectroscopy [14–18]. The high Fe content of Maraging-300 steel means that Mössbauer spectroscopy is a powerful nanometric technique for studying the mobility and redistribution of solute atoms during ageing.

Many authors have used Mössbauer spectroscopy to investigate some types of maraging steel other than Maraging-300, most of them studied only the early stages of ageing. Although many studies have been carried out in the investigation of precipitate formation in Maraging-300 steel, there are no time-temperature-transformation (TTT) curves for this material on literature and there are still many doubts about the precipitation kinetics of this grade of maraging steel. With the aim of obtaining more detailed information about the precipitation kinetics of this steel, in this paper transmission Mössbauer spectroscopy (TMS) – with the aid of X-ray powder diffraction (XRPD), TEM, optical microscopy, and Vickers hardness measurements – has been used to investigate the effect of the configuration of the non-iron atoms on the phase transformation and precipitation behaviour of 300 grade maraging steel. The ageing temperature of 480°C was chosen as the more usual industrial treatment temperature. A wide range of ageing times from 1 to 100 h was investigated.

3.3 Results and discussion

3.3.1 X-ray powder diffraction (XRPD)

The XRPD patterns of samples aged at 480°C for 50 h and 100 h are shown in figure 3.1. Reverted austenite peaks were not identified either in the 50 h aged sample or in those with shorter ageing times – including the solution-treated specimen – showing a monophasic martensitic (α') diffraction pattern, in accordance with other studies [7]. Even considering the resolution limits of XRPD, some small extra peaks corresponding to the formation of a secondary phase (γ) were found in the specimen that was aged for 100 h. Using the direct comparison method presented by Cullity [19] and taking into account the equal values in the scattering factors for austenite (γ) and martensite (α') phases for maraging it was possible to estimate the volume fraction of austenite as 2% at this condition.

Figure 3.1 - XRPD patterns of Maraging-300 steel aged at 480°C for 50 and 100 h.

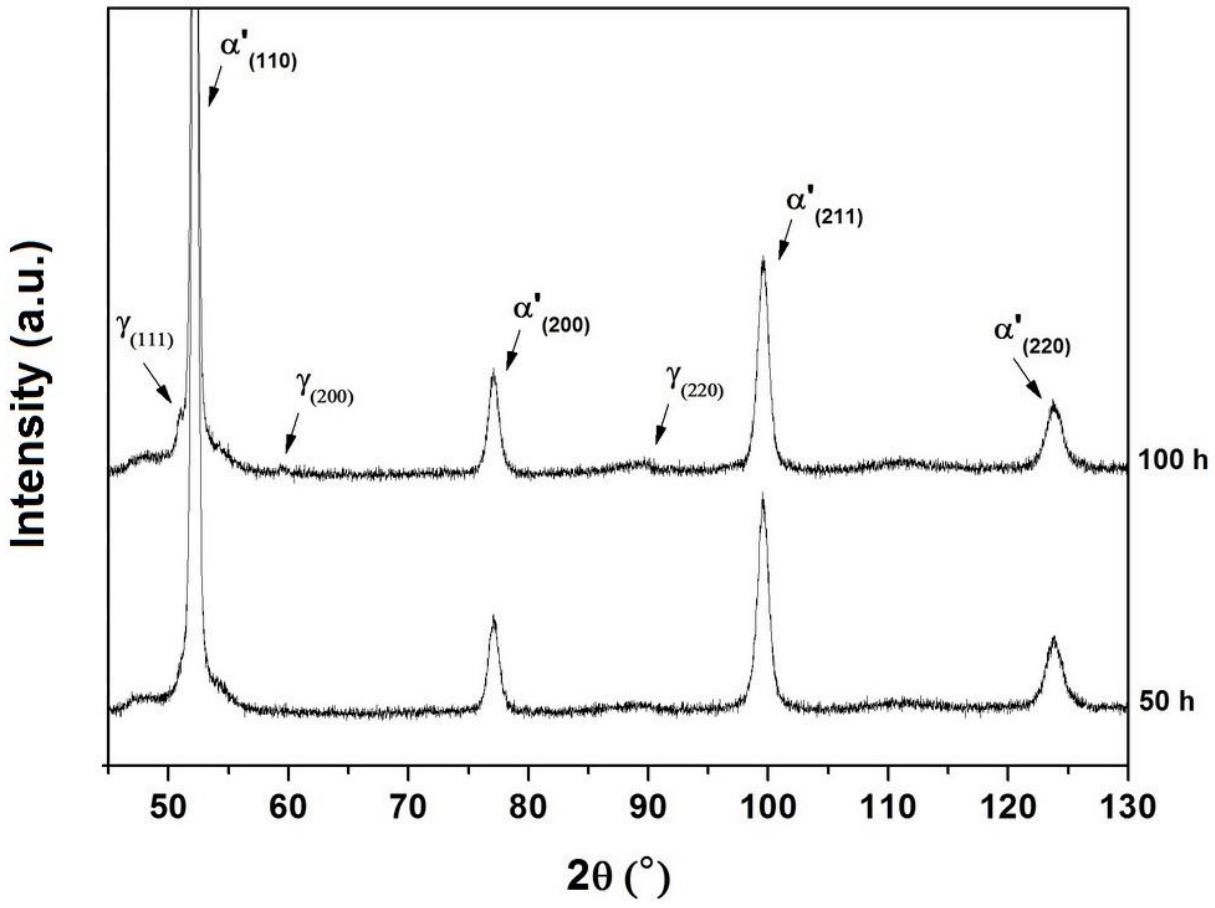

Source: Own author.

The formation of reverted austenite at this temperature is somewhat intriguing, since this phase is not expected at this ageing temperature. However, thermochemical calculation results suggest the formation of some austenite on its final equilibrium state. Due to the long ageing time it is perfectly possible the existence of this phase since in maraging steels the higher the temperature and the longer the ageing time, the more likely the formation of austenite will be. Reverted austenite is known to be a Ni-rich phase. Previous studies [3,4] have reported the Ni_3(Ti,Mo) intermetallic compound as being the first to be formed, followed by Mo-rich phases for longer ageing times. In extremely long ageing times it is most likely that the reverted austenite will be formed from the dissolution of the remaining Ni_3(Ti,Mo) precipitates.

Due to the low volume fraction of precipitates, they cannot be detected by X-ray analysis, but the precipitation of intermetallic compounds containing the main alloying elements will be directly reflected in the lattice constant values of the martensitic matrix. By using the extrapolation method suggested by Cullity [19] and taking into account only the $K\alpha_1$ line, the lattice constant of martensite at each condition was computed and is plotted in figure 3.2.

This parameter decreases fast at the first hour of ageing and then slows down. The lattice constant change reflects that a certain amount of precipitate forming elements – for instance Mo and Ti, that have larger atomic radius than Fe atoms – leave the martensitic matrix. The value of the lattice constant continues to drop until 10 h of ageing. After this the lattice constant changes were not significant, suggesting that most of the atomic rearrangement occurs outside the matrix and that the composition of the martensitic phase becomes more and more constant.

Figure 3.2 - Lattice constant curve of Maraging-300 steel solution-treated and aged at 480°C.

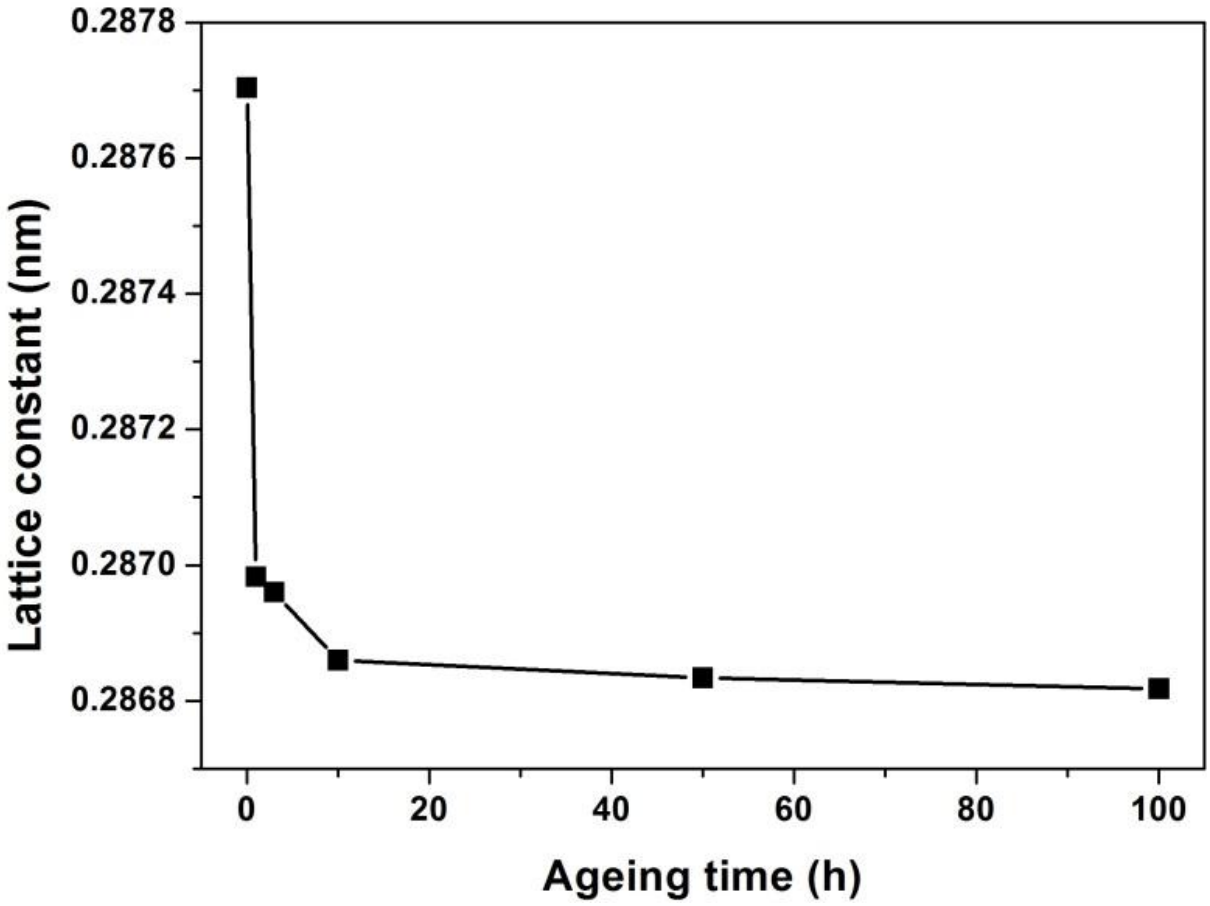

Source: Own author.

3.3.2. Mössbauer analysis

Figure 3.3 shows the Mössbauer spectra of both the solution-treated samples and those aged for various times at 480°C. In order to obtain a more realistic analysis, a distribution fitting was used for this work. A hyperfine field distribution and in some cases a singlet were used for best fitting. A magnetic behaviour is presented in all of them, besides a paramagnetic contribution that increases from 3 h of ageing. The distribution belongs to the martensitic phase. The singlet suggests that there is a paramagnetic phase (or phases) containing a fraction of Fe in these four specimens. Since austenite was detected only at longer ageing times at this temperature, this paramagnetic peak is likely due to the precipitation of intermetallic compounds that contain some Fe.

The paramagnetic phase(s) account for about 4% of the total Fe in the specimens aged for 10 h, a value that increases to about 6% after ageing for 50 h. This suggests that some austenite (superimposed singlets) may be present from 50 h

of ageing, but because of its extremely low volume percentage, it is not detectable by XRPD. Another possibility is the formation of a second type of precipitate that contains Fe as a main compositional element, in this case Fe_2Mo (Laves) and/or Fe_7Mo_6 (μ) phases – as reported by Sha et al. [3] for longer ageing times and higher temperatures.

Figure 3.3 -Mössbauer spectra of Maraging-300 steel solution-treated at 820°C for 30 min and aged at 480°C for various times: (a) as solution-treated; (b) 1 h; (c) 3 h; (d) 10 h; (e) 50 h; (f) 100 h.

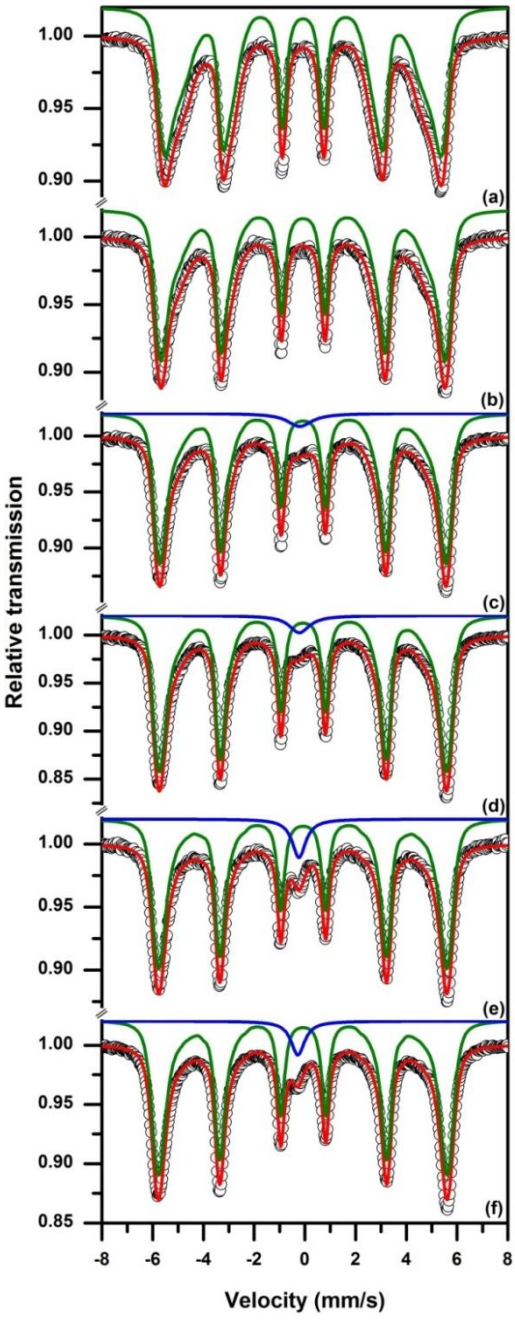

Source: Own author.

The fractional areas for all samples are summarised in table 3.1. There is a small decrease in singlet fractional area when aged for 100 h. At first, this seems unexpected since the amount of both precipitates and austenite commonly increase with time and/or temperature, however the Mössbauer fractional area gives the fraction of Fe atoms in the phase and not the phase fraction. Sha et al. [3] noted that the chemical composition of phases observed in Maraging-300 steel changes in an unpredictable way according to the heat treatment applied. Thus the decrease in singlet fractional area probably occurs due to the migration of Fe atoms back to the martensitic matrix.

Table 3.1 - B_{hf} average value and relative areas for the solution-treated and aged steel samples.

Sample		**Site**	**B_{hf}Avg. (T) (±0.1)**	**Area (%) (±0.5)**
Solution-treated		B_{hf} Dist.	31.7	100
		Singlet	-	-
480°C	1 h	B_{hf} Dist.	33.1	100
		Singlet	-	-
	3 h	B_{hf}Dist.	33.8	96.1
		Singlet	-	3.9
	10 h	B_{hf}Dist.	34.1	95.8
		Singlet	-	4.2
	50 h	B_{hf}Dist.	34.3	93.6
		Singlet	-	6.4
	100 h	B_{hf}Dist.	34.3	94.5
		Singlet	-	5.5

Source: Own author.

As expected for a Fe^0 metallic alloy, the isomer shift (δ) of martensite is close to zero. Because of the low carbon content of this steel, quadrupole splitting (2ε) is also nearly zero, evidencing an irrelevant tetragonal distortion of martensite in this case. The line width of the singlet decreases with time. This is an indication of a reduction in the number of configurations around paramagnetic Fe sites as ageing proceeds.

The probability distribution curves of the magnetic hyperfine field (B_{hf}) for all samples are shown in figure 3.4. The graphics show a notable change at both high and low hyperfine field regions in the initial stages of ageing, suggesting an intense atomic rearrangement for the first 3 h. This is in accordance with the results in figure 3.2 and corroborates that the formation of the intermetallic compounds is in

progress. After ageing for 3 h, the hyperfine field region changes slow down, indicating that atomic redistribution is becoming complete.

Figure 3.4 -Probability distribution curves of the magnetic hyperfine field of Maraging-300 steel solution-treated and aged at 480°C for various times.

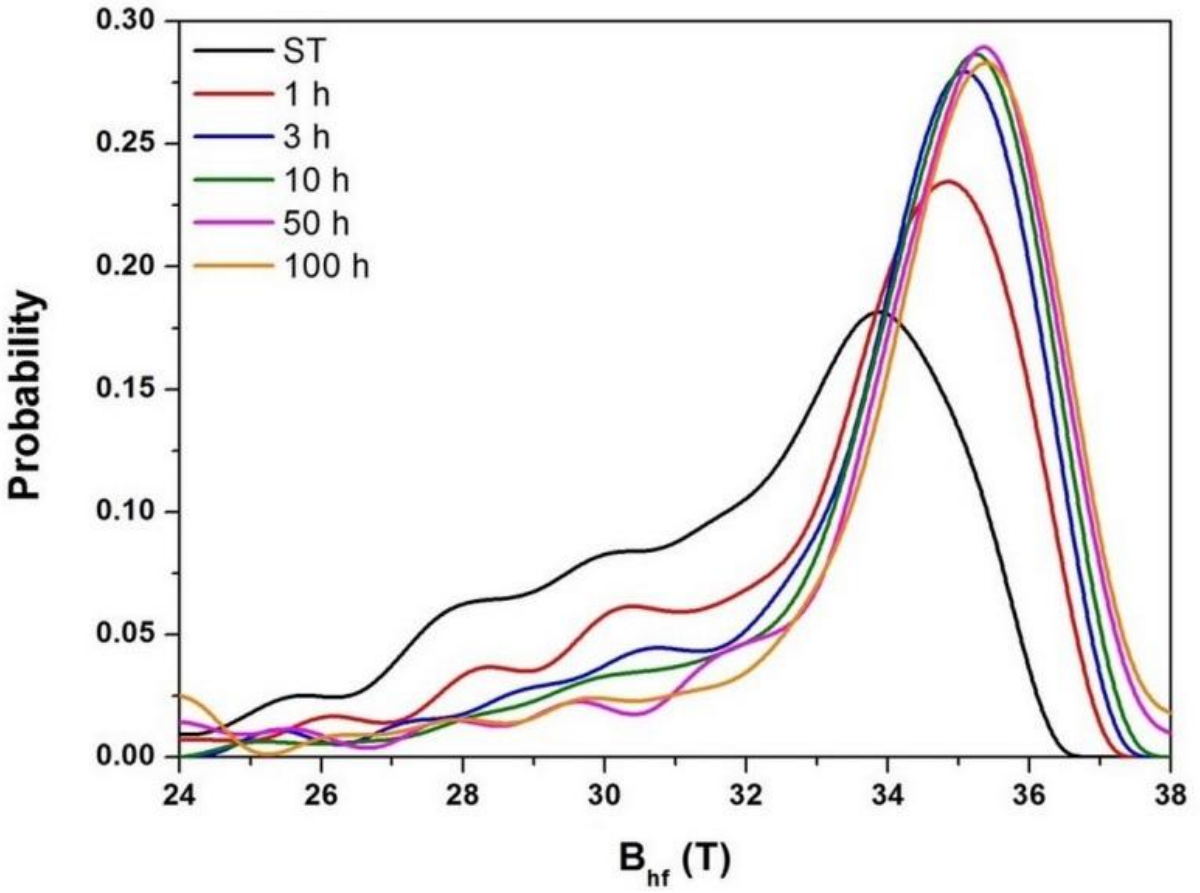

Source: Own author.

The initial severe changes at high and low hyperfine field regions are related to atomic alterations at the first coordination spheres around iron sites. Experiments of Vincze and Campbell [20] pointed out that while Ni and Co have a positive contribution, Mo and Ti have the opposite effect on the magnetic hyperfine field of a ^{57}Fe nucleus. In maraging steel, Co cannot form intermetallic compounds. This B_{hf} behaviour can be explained by the output of alloying elements from the martensitic matrix – in this case Ni, Mo, and Ti – to form precipitates, creating Fe-Co and Ni-Mo-Ti rich zones. The displacement of the B_{hf} average value (see table 3.1) towards the high hyperfine field region confirms this information.

The main intermetallic compounds are limited by the concentration of Ti and Mo, thus the amount of Ni that leaves the martensitic matrix to form precipitates

with these alloying elements is compensated by a higher Co concentration around iron sites. Besides this, the absolute value contributions of Mo and Ti (−3.87 and −1.91 T) to B_{hf} are higher than the Ni contribution (0.94 T) at the first coordination sphere, for example, thus being an addictive effect to increase B_{hf}. This agrees with the observations of Sha et al. [3] who observed the A_3B type precipitate formation when studying the same material aged at 510°C. Tewari et al. [4] also reported the formation of $Ni_3(Ti,Mo)$ at the early stages of ageing in Maraging-350 steel.

As the singlet appears only at ageing times longer than 3 h, two phenomena can be cited to explain this. The first would be that there are still no precipitates in Maraging-300 steel when aged for 1 h. In this way the strengthening of the material comes from Fe-Co-rich and Ni-Mo-Ti-rich zones and not from precipitates, as suggested by Li et al. [16]. The second alternative would be that Fe dissolution into precipitates begins only after 1 h of ageing, suggesting that intermetallic compounds can exist at 1 h but without Fe atoms on its stoichiometry. In this case it is possible to disregard the formation of precipitates containing Fe – like Fe_2Mo Laves phase, μ-Fe_7Mo_6 or σ-FeTi - at this condition.

3.3.3. Microscopy

In this paper, a short TEM study was performed on the specimens that had been aged for 1, 10 and 100 h. Figure 3.5 shows the selected area diffraction pattern (SADP) of the samples and its correspondent bright-field and dark-field images. The presence of precipitates at the material when aged for 1 h was evidenced, confirming that the strengthening of the material comes from the formation of precipitates without Fe atoms. Finely dispersed nanometer-scale precipitates of the order of 5 to 30 nm were found in all conditions studied.

In maraging steels, intermetallic compounds present some inter-planar spacings that are closely matching each other [21]. This makes the identification of precipitates hard to analyse through TEM. The measured interplanar spacing of the spot 1 plus the results showed in previous sections suggest that the $Ni_3(Ti,Mo)$ is the one that appears at the images of the sample aged for 1 h. The same interplanar spacing was obtained at spot 2. A different interplanar spacing was found in spot 3. The result suggests that a Mo-rich and/or Ni_3Ti precipitate may be present at this condition. Although the latter has not been cited in previous studies for long ageing

times, we cannot exclude the possibility that it exists in this condition. It is readily apparent that small amounts of precipitates are found at the early stages and this volume fraction increases as ageing proceeds, in addition to the increasing coalescence of these precipitates.

Figure 3.5 -SADP obtained from Maraging-300 steel aged at 480°C for 1, 10 and 100 h showing diffraction spots from precipitates and its respective bright-field and dark-field images.

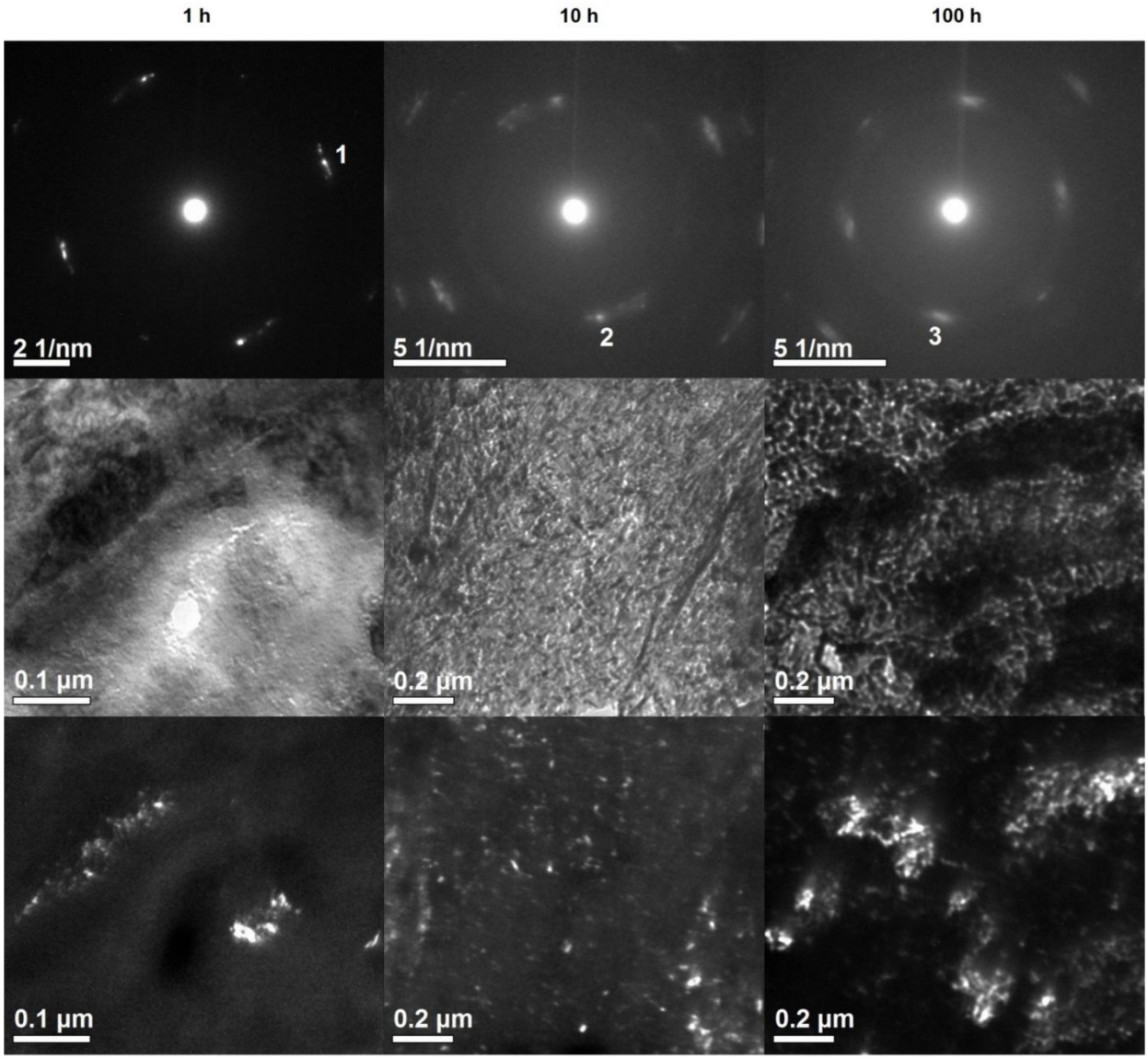

Source: Own author.

Figure 3.6 shows an optical micrograph of the specimen aged for 100 h. A martensitic matrix is seen, and a small fraction of reverted austenite as indicated by the arrows. Austenite particles smaller than 5 µm were found randomly distributed in the material. This compilation of results confirms the coexistence of reverted austenite and at least one kind of intermetallic compound at 100 h of ageing and

reveals that the paramagnetic contribution of this condition (see Figure 3.3) is actually a representation of at least two superimposed singlets.

Figure 3.6 -Optical micrograph obtained from Maraging-300 steel aged at 480°C for 100 h showing small amounts of reverted austenite (indicated by arrows).

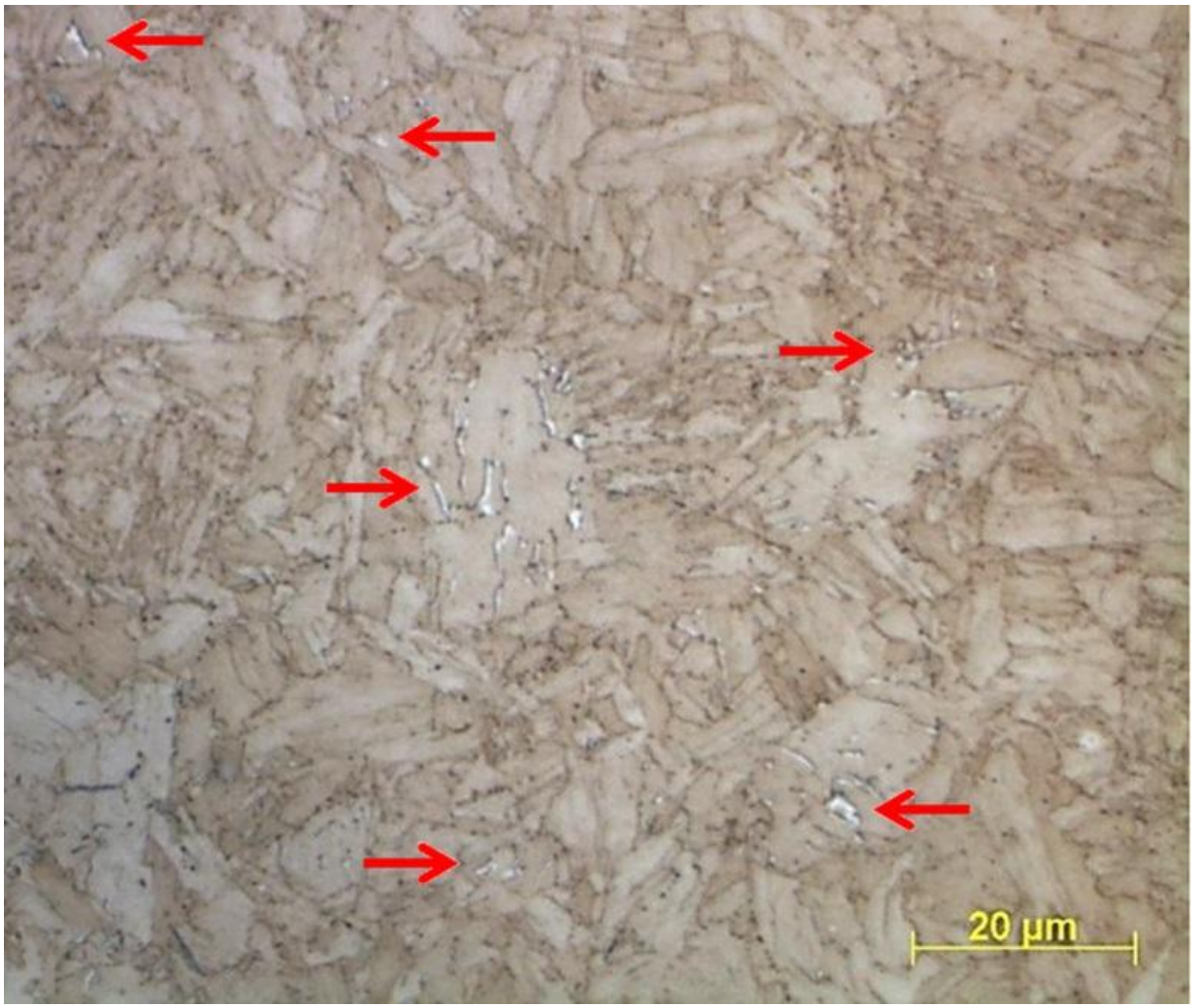

Source: Own author.

3.3.4. Hardness measurements

Figure 3.7 depicts the Vickers hardness results of the samples studied. At this temperature, at least three stages of the hardening process may be defined. The steel presented a fast increase in hardness values at initial ageing times (≤ 1 h), then a continuous slow increase was observed until 50 h of ageing and a small decrease at 100 h.

Figure 3.7 -Age hardening curve of Maraging-300 steel solution-treated and aged at 480°C.

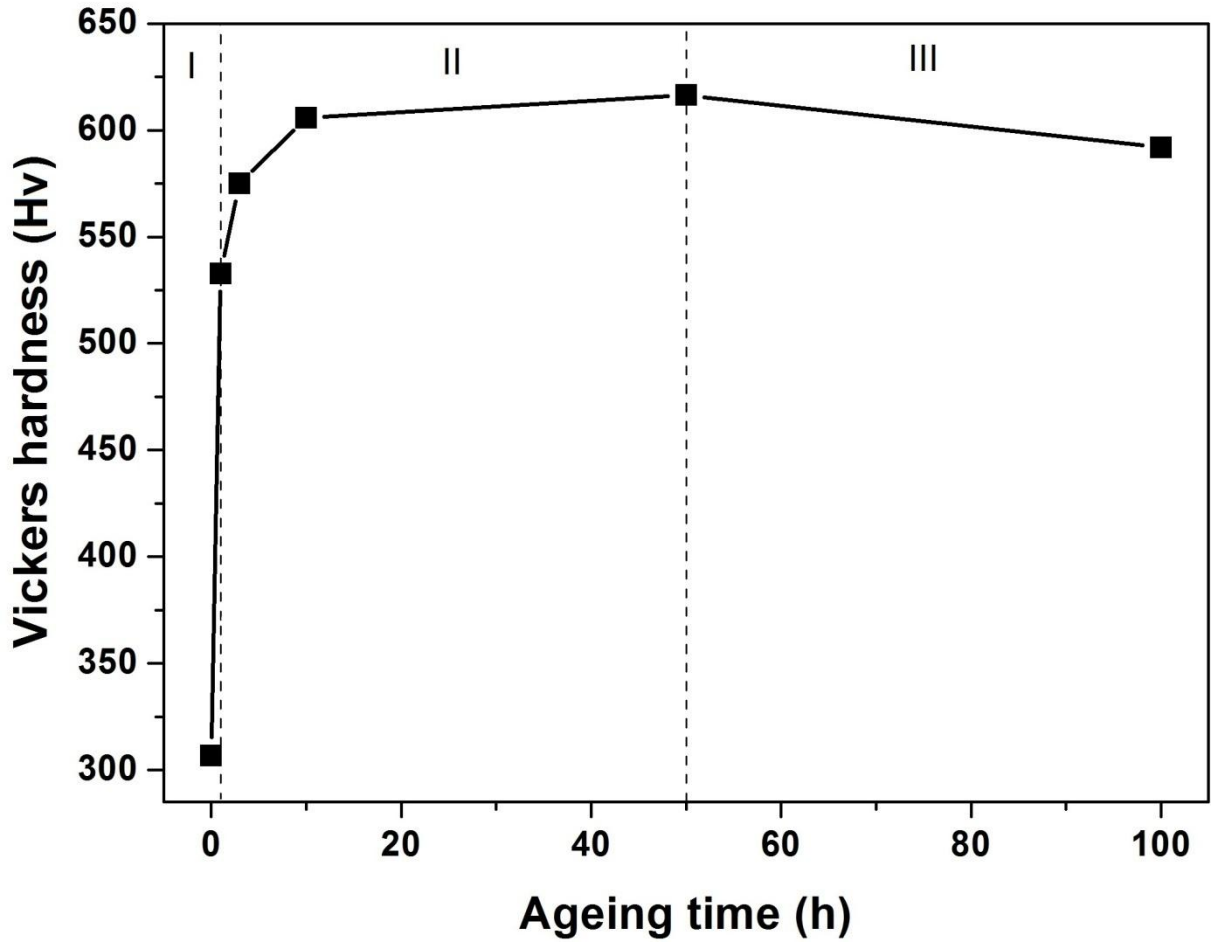

Source: Own author.

All stages are in accordance with the results discussed in previous sections. At the first stage, the strengthening of the material is caused by the distributed precipitates that act as an effective barrier to the motion of dislocations, and also by the distortion of the martensite crystal lattice as a consequence of these precipitates. The initial intense atomic redistribution evidenced in Mössbauer analysis plus the fast decrease of the lattice constant value and the result of the dark-field image for this same condition corroborates this.

At the second stage, the increase in the volumetric fraction of the precipitates is certainly the factor that drives the hardness gain of the material. At this stage, the results presented in previous sections show that Fe-rich precipitates may be present. Due to their morphology and coherence degree with the martensitic matrix, precipitates of this type have a lower influence on the hardness of the material when compared to A_3B types. In addition, as ageing proceeds the precipitate size

increased, precipitate coarsening occurred and interparticle distance also increased, causing a slowdown in the strengthening of the material.

Similarly to the lattice constant, no substantial differences were found between the hardness values of samples aged for between 50 and 100 h. At this final stage a small decrease in hardness was seen. The coalescence of precipitates shown in the sample aged for 100 h can be considered a softening factor that explains this. The final decrease is also most probably related to the fraction of austenite found in this sample by XRPD and optical microscopy.

3.4 Conclusions

The ageing of Maraging-300 steel at 480°C produces the precipitation of intermetallic compounds in a bcc Co-rich martensitic matrix at all conditions studied. Mössbauer and DRX results showed that Ni, Mo and Ti are the main elements that form precipitates and most of the atomic redistribution occurs until 3 h of ageing. After this, most of the atomic rearrangement occurs outside the matrix, between the paramagnetic phases formed and thus the chemical composition of martensite becomes more and more constant. The precipitates formed in the first hour of ageing do not have Fe on its stoichiometry.

Microscopy results evidenced the increasing coalescence of precipitates with ageing time and the co-existence of small amounts of reverted austenite and at least one kind of precipitate at 100 h of ageing. Compilation of results suggests that Ni_3(Ti,Mo) are the precipitates formed at the early stages of ageing (≤ 10 h) and a Mo-rich and Ni_3Ti precipitate may be present at the final condition.

The improving of mechanical properties of the material was evidenced by three stages of the hardening process at this temperature. The first caused by the precipitate formation, the second by the increase in the volumetric fraction of such precipitates and the last by the coalescence of precipitates and the formation of reverted austenite at longer ageing times.

REFERENCES

[1] F. Habiby, T.N. Siddiqui, H. Hussain, A. UlHaq, A.Q. Khan, Lattice changes in the martensitic phase due to ageing in 18 wt% nickel Maraging steel grade 350, J. Mater. Sci. 31 (1996) 305–309.

[2] ASM Specialty Handbook: Nickel, Cobalt, and their alloys. ASM international, 2000, p. 8.

[3] W. Sha, A. Cerezo, G.D.W. Smith, Phase chemistry and precipitation reactions in Maraging steels: Part I. Introduction and study of Co-containing C-300 steel, Metall. Trans. A, 24A (1993) 1221–1232.

[4] R. Tewari, S. Mazumder, I.S. Batra, G.K. Dey, S. Banerjee, Precipitation in 18 wt% Ni Maraging steel of grade 350, Acta Mater. 48 (2000) 1187–1200.

[5] V.K. Vasudevan, S.J. Kim, C.M. Wayman, Precipitation reactions and strengthening behavior in 18 wtpct nickel Maraging steels, Metall. Trans. A, 21A (1990) 2655–2668.

[6] J.M. Pardal, S.S.M. Tavares, M.P. Cindra Fonseca, H.F.G. Abreu, J.J.M. Silva, Study of the austenite quantification by X-ray diffraction in the 18Ni-Co-Mo-Ti Maraging 300 steel, J. Mater. Sci. 41 (2006) 2301–2307.

[7] J.M. Pardal, S.S.M. Tavares, M.P. Cindra Fonseca, M.R. da Silva, J.M. Neto, H.F.G. Abreu, Influence of temperature and aging time on hardness and magnetic properties of the Maraging steel grade 300, J. Mater. Sci. 42 (2007) 2276–2281.

[8] R.F. Decker, Notes on the development of Maraging steels, in: Source book of Maraging steels, 1979, pp. XI–XV.

[9] X.D. Li, Z.D. Yin, H.B. Li, T.C. Lei, M.L. Liu, X.W. Liu, M.Z. Jin, Mössbauer study of the early stages of aging in 18Ni (350) Maraging steel, Mater. Chem. Phys. 33 (1993) 277–280.

[10] N. Bouzid, C. Servant, O. Lyon, Anomalous small-angle X-ray scattering from a Maraging alloy during martensiteunmixing, Phil. Mag. B, 57 (1988) 343–359.

[11] C. Servant, N. Bouzid, A comparative analysis of the precipitation phenomena occurring in Ni and MnMaraging alloys using small-angle neutron scattering experiments, Phil. Mag. B, 60 (1989) 659–687.

[12] Y. Okada, J. Endo, T. Nakayama, Identification of the precipitates in Maraging steels by non-aqueous electrolyte extraction method, Tetsu-to Hagané 69 (1983) 703–710.

[13] K.D. Moore, P.L. Jones, H.F. Cocks, A positron annihilation study of the precipitation hardening effects in a Maraging steel, Phys. Status Solidi (a) 72 (1982) K223–K227.

[14] Z.D. Yin, X.D. Li, M.Z. Zheng, M.L. Liu, X.W. Liu, M.Z. Jin, Mössbauer study of the early stages of ageing in an Fe-19Co-14Mo-10Ni Maraging steel, J. Mater. Sci. Lett. 12 (1993) 179–181.

[15] X. Li, Z. Yin, Mössbauer study of the aging behavior of 18Ni(350) Maraging steel, Mater. Lett. 24 (1995) 235–238.

[16] X. Li, Z. Yin, H. Li, Mössbauer study of the 430 °C decomposition of 18Ni (350) Maraging steel, J. Mater. Sci. Lett. 15 (1996) 314–316.

[17] G.C.S. Nunes, P.W.C. Sarvezuk, V. Biondo, M.C. Blanco, M.V.S. Nunes, A.M.H. Andrade, A. Paesano Jr., Structural and magnetic characterization of martensitic Maraging-350 steel, J. Alloy. Compd. 646 (2015) 321–325.

[18] G.C.S. Nunes, P.W.C. Sarvezuk, T.J.B. Alves, V. Biondo, F.F. Ivashita, A. Paesano Jr., Maraging-350 steel: Following the aging through diffractometric, magnetic and hyperfine analysis, J. Magn. Magn.Mater. 421 (2017) 457–461.

[19] B.D. Cullity, Elements of X-ray diffraction, second ed., Addison-Wesley Publishing Company, Massachusetts, 1956.

[20] I. Vincze, I.A. Campbell, Mössbauer measurements in iron based alloys with transition metals, J. Phys. F: Met. Phys. 3 (1973) 647–663.

[21] W. Sha, A. Cerezo, G.D.W. Smith, Phase chemistry and precipitation reactions in Maraging steels: Part IV. Discussion and conclusions, Metall. Trans. A, 24A (1993) 1251–1256.

4 AN ATOMIC REDISTRIBUTION STUDY OF THE 440°C AGEING KINETICS IN MARAGING-300 STEEL

4.1 Review

Mössbauer spectroscopy, X-ray diffraction and hardness measurements were used to investigate the atomic redistribution and phase transformation of solution-treated and 440°C aged Maraging-300 steel specimens. The ageing temperature that resulted in the best mechanical properties in this steel was 480°C. At 440°C, the formation of the precipitates that assure excellent mechanical properties of the maraging steel (Ni_3Ti, Fe_2Mo) was not expected. The results indicated that Mo and Ti redistribution was severe during the first hour of ageing. The mobility of the Ni atoms probably occurred during all stages of the ageing process, and the Co atoms remained close to Fe atomic sites. An irregular behaviour of the formation of paramagnetic phases containing iron was observed, and some evidence of the formation of these phases without Fe will be discussed. The formation of metastable phases was suggested and the possibility of austenite reversion was not discarded at this ageing temperature.

4.2 Introduction

Maraging steels are a class of Fe-based alloying steels that are age-hardened by the precipitation of finely dispersed intermetallic compounds in a low-carbon martensitic matrix. The combination of appropriate mechanical and magnetic properties makes it a suitable material for strategic applications in the aeronautical, aerospace and nuclear industries.

The main alloying elements in this steel are Ni, Co, Mo and Ti. Carbon is considered an impurity, and the high nickel content (18 wt% Ni) ensures that martensite (α′) forms on air cooling [1]. The low carbon bcc martensitic matrix is hardened by fine-scale precipitation of intermetallic compounds, such as the needle-like $Ni_3(Ti,Mo)$ η-phase. Other phases, like the A_3B X-phase, A_2B ω-phase, A_8B S-phase, Fe_7Mo_6 μ-phase and Fe_2Mo Laves phase (longer ageing time) were also reported in early studies on 300 and 350 grade maraging steels at low ageing

temperatures [2,3]. Reversion to austenite (γ) was also noticed at higher temperatures and for longer ageing times [4-6].

Thermal processing of maraging steels commonly involves a solution treatment at 820°C (minimum temperature) for at least 30 min, and an ageing process at temperatures of 400–650°C, inducing the formation of intermetallic compounds through the redistribution of atoms. The nanometric structure of the precipitates makes them hard to analyse. Because of this, a variety of techniques have been used to study their precipitation behaviour, including: transmission electron microscopy (TEM) [4], small angle X-ray scattering (SAXS) [7], small angle neutron scattering (SANS) [8], electrolyte extraction method [9], positron annihilation [10] and Mössbauer spectroscopy [11-15]. Since Maraging-300 steel has about 66 wt% Fe, Mössbauer spectroscopy becomes a powerful local technique for studying the mobility and redistribution of solute atoms during ageing.

Some authors [11-13] studied the early stages (≤ 1 h) of the ageing process of both Maraging-350 and a Fe-19Co-14Mo-10Ni maraging steel using Mössbauer spectroscopy. They analysed samples aged at 500°C for times varying between 2 and 60 min. It was reported that the redistribution of atoms was fast in the initial stages of ageing and then slowed down. Nunes et al. [14] used Mössbauer spectroscopy to study samples aged at various temperatures above 480°C and longer ageing times (≤ 12 h). Li et al. [15] studied the decomposition of Maraging-350 at low ageing temperature (430°C). The latter did not find paramagnetic components in the Mössbauer spectra until 4 h of ageing, and suggested that the embrittlement of 18Ni(350) maraging steel aged between 400 and 450°C results from Fe-Co-rich and Ni-Mo-Ti-rich zones, and not from precipitates.

Many authors have studied Maraging-350 steel through Mössbauer spectroscopy, but there are few studies that investigated Maraging-300 steel, and fewer at the low ageing temperatures using this technique. In addition, the exact nature of the precipitation behaviour at these conditions is still uncertain. In this paper, transmission Mössbauer spectroscopy (TMS), with the aid of X-ray powder diffraction (XRPD) and Vickers hardness measurements, was used to investigate the effect of the atomic redistribution of the non-iron atoms on the ageing kinetics of 300 grade maraging steel aged at 440°C.

4.3 Result and Discussion

4.3.1 X-ray powder diffraction (XRPD)

The XRPD patterns of both the solution-treated and all aged samples are shown in Figure 4.1. Reverted austenite peaks were not identified, resulting in a monophasic martensitic diffraction pattern, as expected for this temperature according to previous studies [6,16]. Due to the very low volume fraction of precipitates, they cannot be identified by X-ray analysis. No significant changes were observed in the diffractograms from the solution-treated condition until 100 h of ageing.

Figure 4.1 -XRPD patterns of solution-treated and aged Maraging-300 steel specimens.

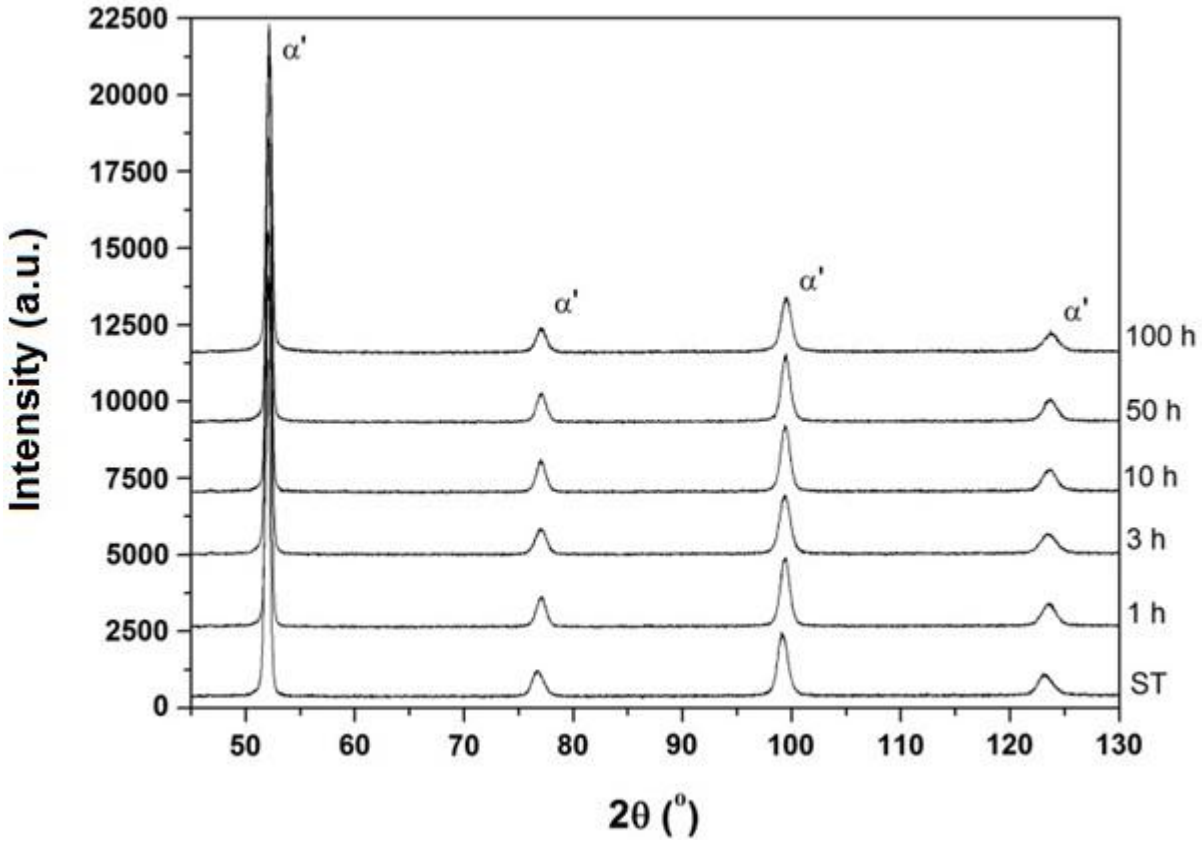

Source: Own author.

The variation of the bcc martensitic lattice constant value was completely attributed to the atomic redistribution of alloying elements as the ageing proceeded. The zone formation of alloying elements, or intermetallic compound precipitation, or even the reversion of austenite in quite small amounts (below the resolution limits of XRPD) will be directly reflected in lattice constant values of the martensitic matrix.

For this paper, the martensite lattice constant at each condition was computed using the extrapolation method suggested by Cullity [17] and taking into account only the $K\alpha_1$ line and is plotted in Figure 4.2. The value of this parameter decreased quickly during the first hour of ageing, and became a bit smaller after 10 h.

Figure 4.2 -Age hardening and bcc martensitic lattice constant values of solution-treated and aged Maraging-300 steel specimens.

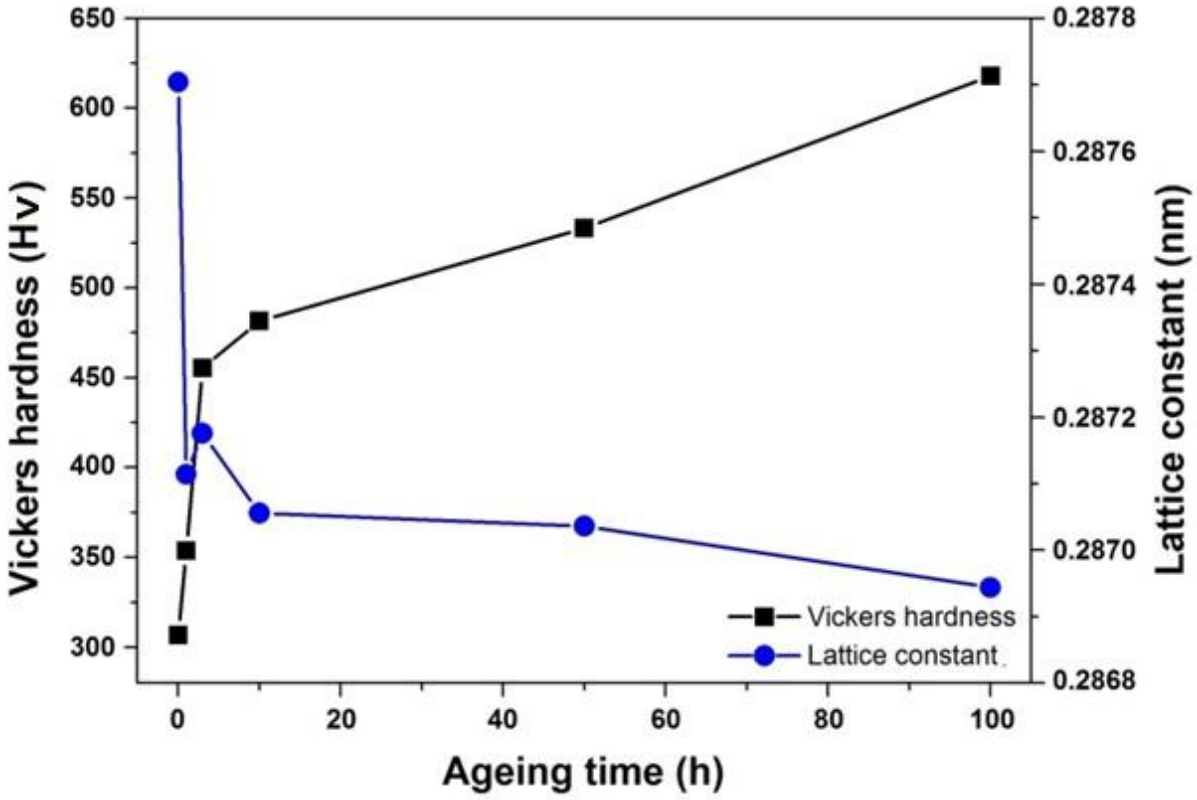

Source: Own author.

When a certain amount of alloying elements leaves the martensitic matrix to form other phases, their positions are occupied by other atoms of different atomic volume [18]. This fact implies a change in the unit cell volume of Fe-rich bcc martensite, and therefore in its lattice constant. Note that Mo and Ti atoms are much larger than Fe atoms, whereas Ni and Co atoms are a little bit smaller. The lattice constant change reflects that a certain amount of alloying elements, most likely Mo and Ti, leaving the martensitic matrix, mainly during the first hour of ageing. After this, the Mo and Ti output slowed down. In Maraging-300 steel, Co does not form precipitates itself and only substitutes a few percent of Ni and Fe in Ni_3Ti and Fe_7Mo_6 intermetallic phases, respectively [19]. The amount of Ni that leaves the martensitic matrix to form paramagnetic phases with other alloying elements is compensated by

a higher Co concentration around Fe sites, and then no relevant changes can be noted in lattice constant value because of this Ni and Co rearrangement. This is a reasonable explanation for the lattice constant curve behaviour. Thus, there is a possibility that Ni left the martensitic matrix in all stages of ageing on this study.

4.3.2 Hardness measurements

Vickers hardness of all samples is also shown in Figure 4.2. At this temperature, two stages of the hardening process may be defined. The steel presented a fast increase in hardness values at initial ageing times (≤ 3 h), and then a continuous slow increase was observed until 100 h of ageing. As in the studies of Lecomte et al. [20] and Servant and Bouzid [21], the over-ageing phenomenon did not occur at this temperature until 100 h of ageing.

Finely distributed precipitates present an effective barrier to the motion of dislocations [22]. Precipitate size, shape and spacing seem to be very relevant factors in the age hardening mechanism of the material. Following Magnée et al. [3], the hardening that results from holding at temperatures below 450°C is probably due to the formation of ordered precipitates, 1 to 5 nm in diameter, that are coherent with the martensitic matrix. This coherency indicates that at initial stages of ageing at this temperature, strengthening is related to the stress required for dislocations to cut through precipitates. This result in higher hardness values due to the increase in shear stress required to cut through the precipitates, in addition to the stress generated in the matrix by the simple presence of precipitated phase particles.

Tewari et al. [2] reported the formation of metastable phases in Maraging-350 when aged at low temperatures. Thus, in the present study, with increasing ageing time at this temperature, the formation of increasingly strong precipitate particles (different phases) can occur, enabling Orowan's mechanism and greatly hindering the dislocation movement in the material. In this case, the formation of successive phases finely dispersed in the steel occurred until equilibrium was reached, as the phases formed.

As the ageing proceeded (> 3 h), the precipitate size increased, precipitate coarsening occurred and interparticle distance also increased, causing a slowdown in the strengthening of the material. The progressive formation of incoherent particles

with the matrix was an additional fact to explain this. The hardness curve behaviour in Figure 4.2 reflects this.

Despite the notable strength gain of the material at this temperature in the initial stages of ageing (≤ 3 h), the hardness values found at these conditions were relatively lower than those found at higher ageing temperatures (i.e. at 480°C). This suggests that the precipitates that formed during these ageing stages at this temperature would not be the same as found at higher temperatures. However, for longer ageing times, the hardness behaviour found in this study was similar with previous results [6] reported for maraging steels.

4.3.3 Mössbauer analysis

The Mössbauer spectra of the solution-treated sample and those aged for various times at 440°C are shown in Figure 4.3. A hyperfine field distribution, and in some cases a singlet, were used for best fitting. A ferromagnetic behaviour was observed in all of them, other than a paramagnetic contribution at 3 and 50 h of ageing. The distribution belongs to the martensitic phase. The singlet suggests that there is a paramagnetic phase (or phases) containing a fraction of Fe in these two specimens. This paramagnetic peak is likely due to the precipitation of intermetallic compounds that contain some Fe. However, although the reversion of austenite is not common at this temperature for maraging steels and was not detected by XRPD at this work, the presence of austenite in quite small amounts cannot be excluded in this case.

The paramagnetic phase(s) accounted for about 1.59 and 1.31% of the total Fe in the specimens aged for 3 and 50 h, respectively. For the sample aged for 10 h, the presence of a singlet for fitting the results may be possible. However, with values so small that they can be considered within the margin of error, this possible singlet was disregarded in this work. This irregular behaviour of paramagnetic phase(s) suggests the formation of metastable paramagnetic precipitate (or precipitates) that contains Fe as a compositional element. This is in accordance with what was discussed in the previous section.

As the paramagnetic peak was not detected for the samples aged for 1, 10 and 100 h, it is reasonable to think that intermetallic compounds that contain Fe did not exist at these conditions. This is an important result, because it showed that Fe

containing phases like Fe_2Mo Laves or Fe_7Mo_6 μ-phase did not exist at these ageing times. This is not in agreement with what was found for Maraging-350 by Tewari et al. [2], who suggested the existence of Fe_2Mo Laves phase after ageing for about 45 h at this temperature. According to Sha et al. [19], the activity of Mo is raised by the presence of Co in maraging steels. Therefore, the driving force for the precipitation of Mo-rich phases is increased. The higher amount of Co for Maraging-350 steel explains the difference in Mo-rich phase kinetics for these two grades of maraging steels.

Figure 4.3 -Mössbauer spectra of Maraging-300 steel solution-treated at 820°C for 30 min and aged at 440°C for various times: (a) as solution-treated; (b) 1 h; (c) 3 h; (d) 10 h; (e) 50 h; (f) 100 h.

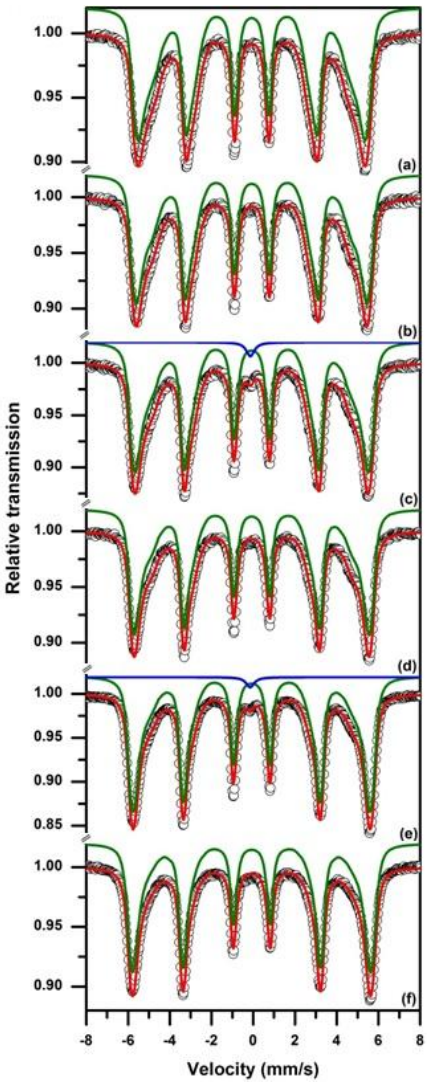

Source: Own author.

As expected for a Fe^0 metallic alloy, the isomer shift (δ) of martensite was close to zero. Because of the low carbon content of this steel, quadrupole splitting (2ε) was also close to zero, confirming that the martensitic matrix can be considered as bcc in this case. The sextet linewidth decreased from Figure 4.3 (a) to (f), indicating a reduction in the number of configurations around ferromagnetic Fe sites as ageing proceeds.

The probability distribution curves of the magnetic hyperfine field (B_{hf}) for all samples are shown in Figure 4.4. The graphics show a notable continuous change at both high and low hyperfine field regions until 100 h of ageing, suggesting that an intense atomic rearrangement occurred at all ageing stages. The continuous severe changes at low and high hyperfine field regions were related to atomic alterations at the first coordination spheres around iron sites. Experiments by Vincze and Campbell [23] pointed out that while most of the chemical elements, including Mo and Ti, have a negative contribution (-3.87 and -1.91 T at the first coordination sphere), Ni and Co have the opposite effect (0.94 and 1.33 T) on the magnetic hyperfine field of a ^{57}Fe nucleus. As Co does not form precipitates itself, this B_{hf} behaviour can be explained by a continuous output of alloying elements from the martensitic matrix – in this case Ni, Mo, and Ti – to form paramagnetic phases, creating Fe-Co and Ni-Mo-Ti rich zones. The fact that the absolute value contributions of Mo and Ti to B_{hf} were higher than the Ni contribution is an addictive effect to explain the displacement of the B_{hf} average value (see Figure 4.4) towards the high hyperfine field region. As the Co contribution to B_{hf} is higher than Ni contribution, an additional effect occurs when Co atoms replace previous Ni atoms sites. This is in agreement with the results discussed in the X-ray section, and the same explanation about Mo, Ti and Ni atom mobility in all stages of ageing can be applied here.

The highest probability values at each condition were related to the increasing values of B_{hf}, and all of them were always higher than the magnetic hyperfine field expected for α-Fe. This suggests that Fe sites for the ferromagnetic martensite were more and more surrounded by alloying elements with positive contribution to its B_{hf} – in this case Ni and mainly Co – as ageing time increased.

Although the singlet appears only at some of the ageing times, there is some evidence that precipitation (without Fe atoms) occurred continuously besides

these ageing times, as indicated by the behaviour of the probability distribution curves.

Figure 4.4 - Probability distribution curves of the magnetic hyperfine field of Maraging-300 steel solution-treated and aged at 440°C for various times.

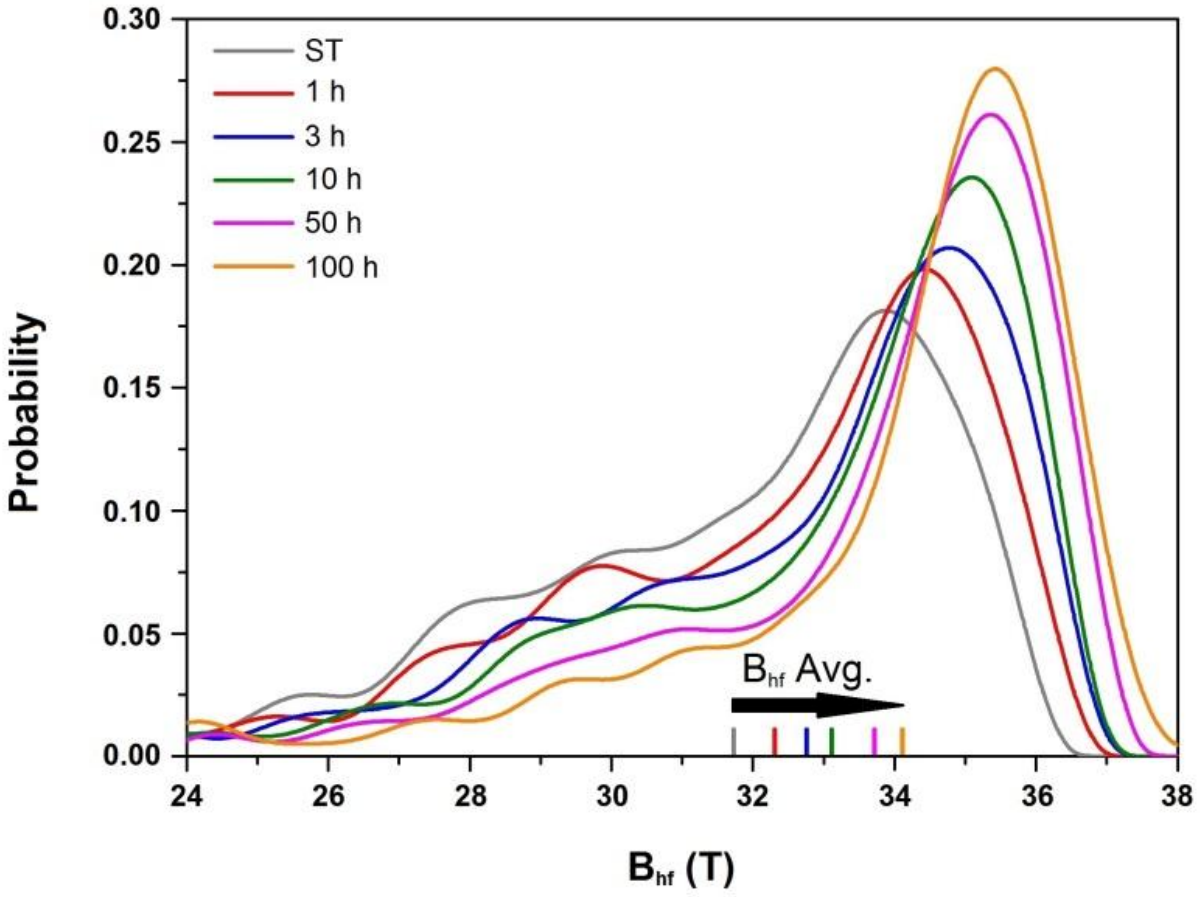

Source: Own author.

4.4 Conclusions

The atomic redistribution of Maraging-300 steel aged at 440°C was intense and occurred continuously until 100 h of ageing. The Mo and Ti atom mobility was severe during the first hour of ageing and then slowed down. The Ni atom mobility likely occurred during all stages of ageing, and the Co atoms remained close to Fe atom sites. Paramagnetic phases, with some amount of Fe, only existed at 3 and 50 h of ageing, and possibly at 10 h. The possibility of formation of quite small amounts of reverted austenite cannot be disregarded at these conditions. Intermetallic compounds containing a fraction of Fe, for instance the Laves or μ-phase, did not exist at 1 and 100 h of ageing. This indicates that Mo atoms probably left the martensitic matrix to form some precipitate other than Laves or μ-phase at

these conditions. Precipitates formed at this temperature were not probably the same as those found at higher ageing temperatures. The compilation of results suggests the formation of metastable phases during all stages of ageing that were investigated in this paper.

REFERENCES

[1] J.R. Davis, ASM Specialty Handbook: Nickel, Cobalt, and their alloys. ASM international; 2000.

[2] R. Tewari, S. Mazumder, I.S. Batra, G.K. Dey, S. Banerjee, Precipitation in 18 wt% Ni maraging steel of grade 350. ActaMaterialia.2000; 48: 1187–1200.

[3] A. Magnée, J.M. Drapier, J. Dumont, D. Coutsouradis, L. Habraken, Cobalt containing high-strength steels. Bruxelles: Centre D´information du Cobalt; 1974.

[4] V.K. Vasudevan, S.J. Kim, C.M. Wayman, Precipitation reactions and strengthening behavior in 18 wtpct nickel maraging steels. Metallurgical and Materials Transactions A. 1990; 21A: 2655-2668.

[5] J.M. Pardal, S.S.M. Tavares, M.P. Cindra Fonseca, H.F.G. Abreu, J.J.M. Silva,Study of the austenite quantification by X-ray diffraction in the 18Ni-Co-Mo-Ti maraging 300 steel. Journal of Materials Science.2006; 41: 2301-2307.

[6] J.M. Pardal, S.S.M. Tavares, M.P. Cindra Fonseca, M.R. da Silva, J.M. Neto, H.F.G. Abreu,Influence of temperature and aging time on hardness and magnetic properties of the maraging steel grade 300. Journal of Materials Science.2007; 42: 2276-2281.

[7] N. Bouzid, C. Servant, O. Lyon,. Anomalous small-angle X-ray scattering from a maraging alloy during martensite unmixing, Philosophical Magazine B. 1988; 57: 343-359.

[8] C. Servant, N. Bouzid, A comparative analysis of the precipitation phenomena occurring in Ni and Mn maraging alloys using small-angle neutron scattering experiments, Philosophical Magazine B. 1989; 60: 659-687.

[9] Y. Okada, J. Endo, T. Nakayama,.Identification of the precipitates in maraging steels by non-aqueous electrolyte extraction method. Tetsu-to-Hagané.1983; 69: 703-710.

[10] K.D. Moore, P.L. Jones, H.F. Cocks, A positron annihilation study of the precipitation hardening effects in a maraging steel. Physica status solidi (a). 1982; 72: K223-k227.

[11] X.D. Li, Z.D. Yin, H.B. Li, T.C. Lei, M.L. Liu, X.W. Liu, M.Z. Jin,Mössbauer study of the early stages of aging in 18Ni(350) maraging steel. Materials Chemistry and Physics.1993; 33: 277–280.

[12] Z.D. Yin, X.D. Li, M.Z. Zheng, M.L. Liu, X.W. Liu, M.Z. Jin,Mössbauer study of the early stages of ageing in an Fe-19Co-14Mo-10Ni maraging steel. Journal of Materials Science Letters.1993; 12: 179-181.

[13] X. Li, Z. Yin,Mössbauer study of the aging behavior of 18Ni(350) maraging steel. Materials Letters.1995; 24: 235-238.

[14] G.C.S. Nunes, P.W.C. Sarvezuk, T.J.B. Alves, V. Biondo, F.F. Ivashita, A. Paesano Jr, Maraging-350 steel: Following the aging through diffractometric, magnetic and hyperfine analysis. Journal of Magnetism and Magnetic Materials.2017; 421: 457-461.

[15] X. Li, Z. Yin, H. Li,.Mössbauer study of the 430 °C decomposition of 18Ni(350) maraging steel. Journal of Materials Science Letters.1996; 15: 314-316.

[16] J.M. Pardal, S.S.M. Tavares, V.F. Terra, M.R. Da Silva, D.R. Dos Santos, Modeling of precipitation hardening during the aging and overaging of 18Ni–Co–Mo-Timaraging 300 steel, J Alloy Compd, 2005; 393:109-113.

[17] B.D. Cullity, Elements of X-ray diffraction, second ed. Massachusetts: Addison-Wesley Publishing Company; 1956.

[18] Z. Guo, D. Li, W. Sha, Quantification of precipitate fraction in Maraging steels by X-ray diffraction analysis.Materials Science and Technology.2004; 20: 126-130.

[19] W. Sha, A. Cerezo, D.D.W. Smith, Phase chemistry and precipitation reactions in maraging steels: Part IV. Discussions and Conclusions. Metallurgical and Materials Transactions A. 1993; 24A: 1251-1256.

[20] J.B. Lecomte, C. Servant, G. Cizeron, A comparison of the structural evolution occurring during anisothermal or isothermal treatments in the case of nickel and manganese type maraging alloys. Journal of Materials Science.1985; 20: 3339-3352.

[21] C. Servant, N. Bouzid, Influence of the increasing content of Mo on the precipitation phenomena occurring during tempering in the Maraging alloy Fe-12Mn-9Co-5Mo. Acta Metallurgica. 1988; 36: 2771-2778.

[22] M.A. Meyers, K.K. Chawla, Mechanical Behavior of Materials. New Jersey: Prentice Hall; 1998.

[23] I. Vincze, I.A. Campbell, Mössbauer measurements in iron based alloys with transition metals. Journal of Physics F: Metal Physics. 1973; 3: 647-663.

5 INVESTIGATION OF PHASE TRANSFORMATION IN MARAGING-300 STEEL AGED ABOVE LITERATURE-RECOMMENDED TEMPERATURE

5.1. Review

Maraging steels are known to achieve the highest strength limit when aged around 480°C. However some research has been carried out in temperatures different from 480°C with the aim of improving the toughness and magnetic properties of the material. In this paper Mössbauer spectroscopy, X-ray diffraction, hardness measurements, and transmission electron microscopy were used to investigate the phase transformation process through atomic redistribution of solution-treated and 520, 560 and 600°C-aged Maraging-300 steel specimens. The results indicated that the precipitation of intermetallic compounds, which are responsible for improvement of mechanical properties, occurs severely and similarly to precipitation at the temperature of 480°C within the first hour of ageing. The coexistence of precipitates and the austenitic phase was detected, and a crystalline/magnetic transition zone was suggested in the material for longer times and higher ageing temperatures.

5.2. Introduction

Maraging steels are a class of ultra-high strength steels that combine high fracture toughness with good magnetic properties. For these reasons Maraging steels are used in the most diverse applications from sports equipment to nuclear, aeronautical and aerospace industries.

Ni, Co, Mo and Ti are the main alloying elements of this steel. On 300 grade maraging steel, some additions of other alloying elements such as Al and Cr in small amounts make the material have about 33 wt% of alloying elements. The low carbon and high nickel content of maraging steels ensures that martensite (α′) forms on air cooling [1], presenting a soft martensitic matrix at the solution-treated condition (usually 820°C for at least 30 min). The strengthening improvement of the material is attained by the precipitation of intermetallic compounds through the redistribution of atoms during the ageing process at the 400–650°C interval. Phases like A_3B X-phase, A_2B ω-phase, A_8B S-phase, Fe_7Mo_6 μ-phase and Fe_2Mo Laves phase (for

longer ageing times) were reported in early studies on 300 and 350 grade maraging steels at low ageing temperatures [2,3]. The $Ni_3(Ti,Mo)$ η-phase and Fe_2Mo Laves phase were found at higher ageing temperatures (> 450°C) [2–5] as well as Ni-rich reverted austenite (γ) for temperatures above 500°C and longer ageing times [5–9].

In maraging steels, the known precipitates present nanometric scale with dimensions between 1 and 50 nm. Besides this, the low volume fraction of such phases makes them hard to analyse. Some authors have tried a variety of techniques to study the precipitation behaviour of maraging steels [6,9–17], most of them studying maraging steels types other than 300 grade at 510°C maximum ageing temperature. The larger particle size as well as higher volume fraction make the reverted austenite easier to analyse, and interesting results can be obtained by conventional methods like X-ray diffraction [7,8]. At high ageing temperatures (> 500°C), the presence of reverted austenite greatly influences the mechanical and magnetic properties of the material. There are few studies that focus on the intermetallic compound precipitation and reversion of austenite at the same time in Maraging-300 steel above 520°C, thus a great number of studies are still required in order to clarify the phase transformation process in the material at these ageing conditions.

In this paper, because of the high Fe content of Maraging-300 steel, transmission Mössbauer spectroscopy (TMS) was chosen as a technique capable of providing valuable information about atomic mobility in this material. X-ray powder diffraction (XRPD), transmission electron microscopy (TEM), and Vickers hardness measurements were used as complementary techniques to investigate the effect of the mobility and configuration of the non-iron atoms on the phase transformation and precipitation behaviour of 300 grade maraging steel aged at 520, 560 and 600°C for times from 1 to 100 h of ageing.

5.3. Results and discussion

5.3.1 X-ray powder diffraction (XRPD)

In maraging steels, due to the very low volume fraction of precipitates, they cannot be detected by X-ray analysis. No reverted austenite peaks were found in the solution-treated sample and in initial stages of ageing at each temperature,

demonstrating a monophasic martensitic diffraction pattern. Figure 5.1 shows the partial XRPD pattern of samples that present the lowest amounts of reverted austenite at each temperature. Some small extra-peaks $(111)_\gamma$ corresponding to the formation of reverted austenite were detected in the specimen aged at 520°C only from 10 h and from 3 h in samples aged at 560 and 600°C respectively. Considering the resolution limits of XRPD, the possibility of reverted austenite existing in residual amounts at earlier ageing times cannot be excluded.

Figure 5.1 - Partial XRPD patterns of Maraging-300 steel showing the lowest amounts of reverted austenite at each ageing temperature.

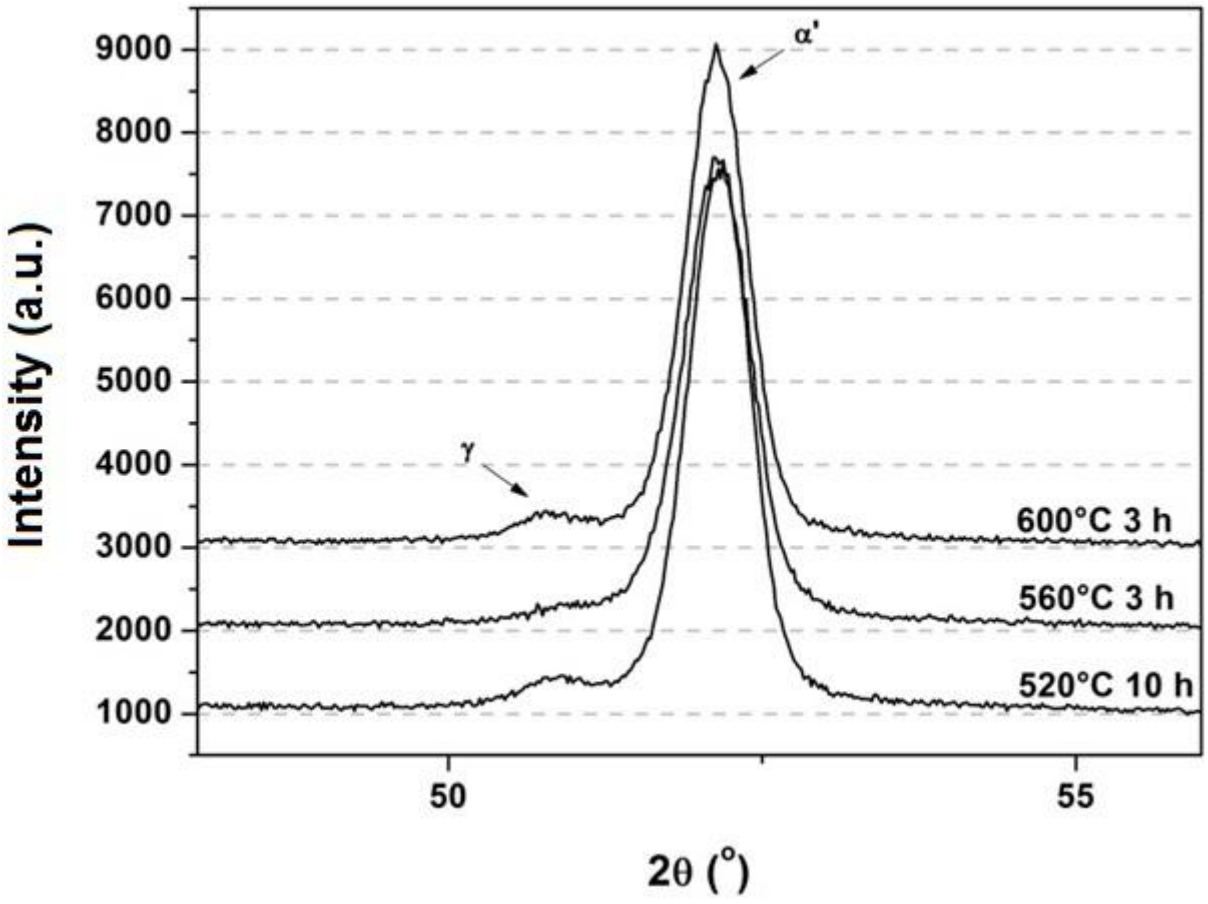

Source: Own author.

Using the direct comparison method presented by Cullity [18], and taking into account the equal values in the scattering factors for austenite (γ) and martensite (α') phases for maraging as suggested by Pardal et al. [7], it was possible to calculate the volume fraction of reverted austenite for all samples, and the results are shown in Figure 5.2. The higher the ageing time and temperature, the higher the volume fraction of reverted austenite. With increasing the ageing time, the slope of

the reverted austenite volume fraction curve decreases, suggesting that the amount of reverted austenite reaches its equilibrium value with prolonged ageing times. In this paper, the maximum amount of reverted austenite (about 54%) was detected at 600°C and 100 h ageing condition.

Figure 5.2 - Age hardening and austenite fraction curves of Maraging-300 steel solution-treated and aged at various conditions.

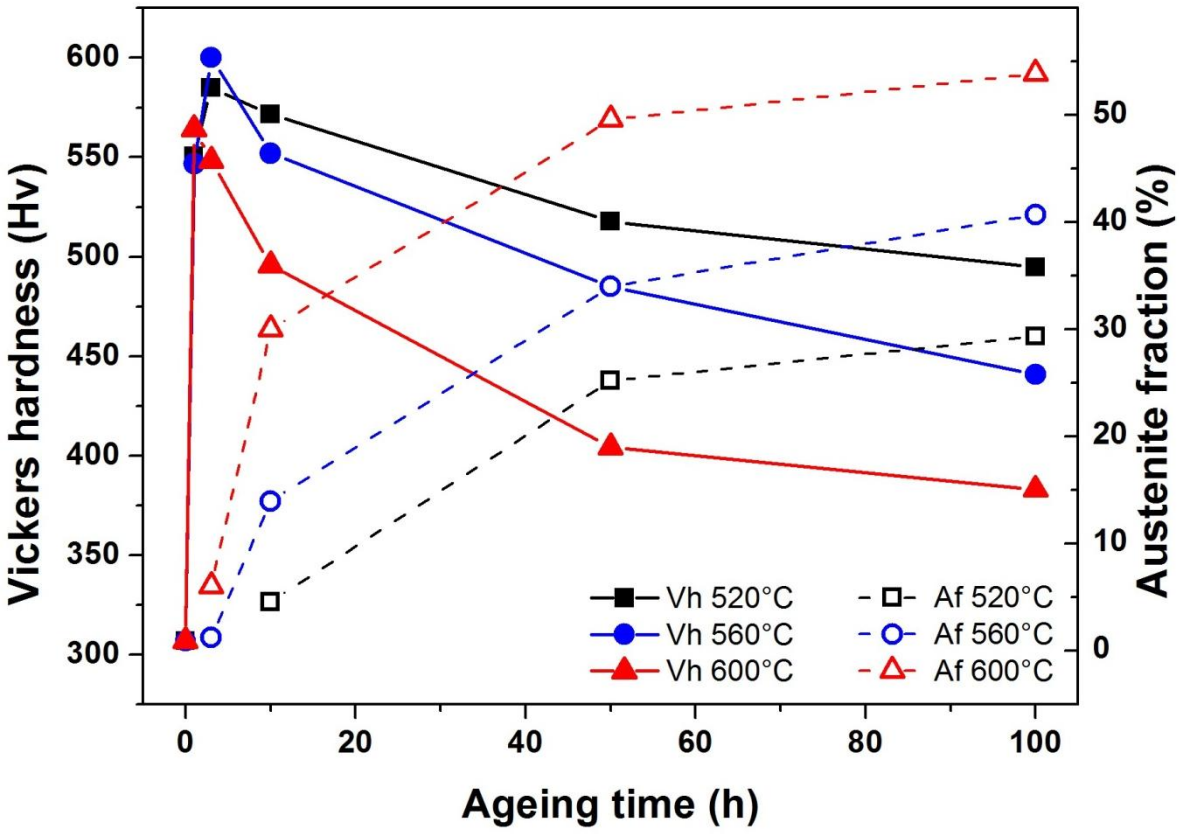

Source: Own author.

By using the extrapolation method suggested by Cullity [18] and taking into account only the $K\alpha_1$ line, the lattice constant curves of the bcc martensitic matrix were computed and are plotted in Figure 5.3. The phase transformation process of Maraging-300 steel will be somehow reflected in the changes of lattice constant values of the bcc martensitic matrix. A fast decrease in lattice constant values is noted for all temperatures at the first hour of ageing. At initial stages of ageing, when most probably there is no reverted austenite, the changes in unit cell volume will be commanded by the formation of precipitates through the atomic redistribution of atoms of the alloying elements. In maraging steels, Mo and Ti atoms are much larger and Ni, and Co atoms are a little bit smaller than Fe atoms. The lattice constant

change indicates that a certain amount of alloying elements, probably most of them Mo and Ti, leaves the martensitic matrix mainly at the first hour of ageing to form precipitates. After the first hour the lattice constant changes were not significant, suggesting that the composition of the martensitic matrix becomes more and more constant. When the nickel-rich reverted austenite begins to form, the alloying elements — mainly Ni — are transferred from the precipitates to be part of the composition of this new phase.

Figure 5.3 -Martensite lattice constant curves of Maraging-300 steel solution-treated and aged at various conditions.

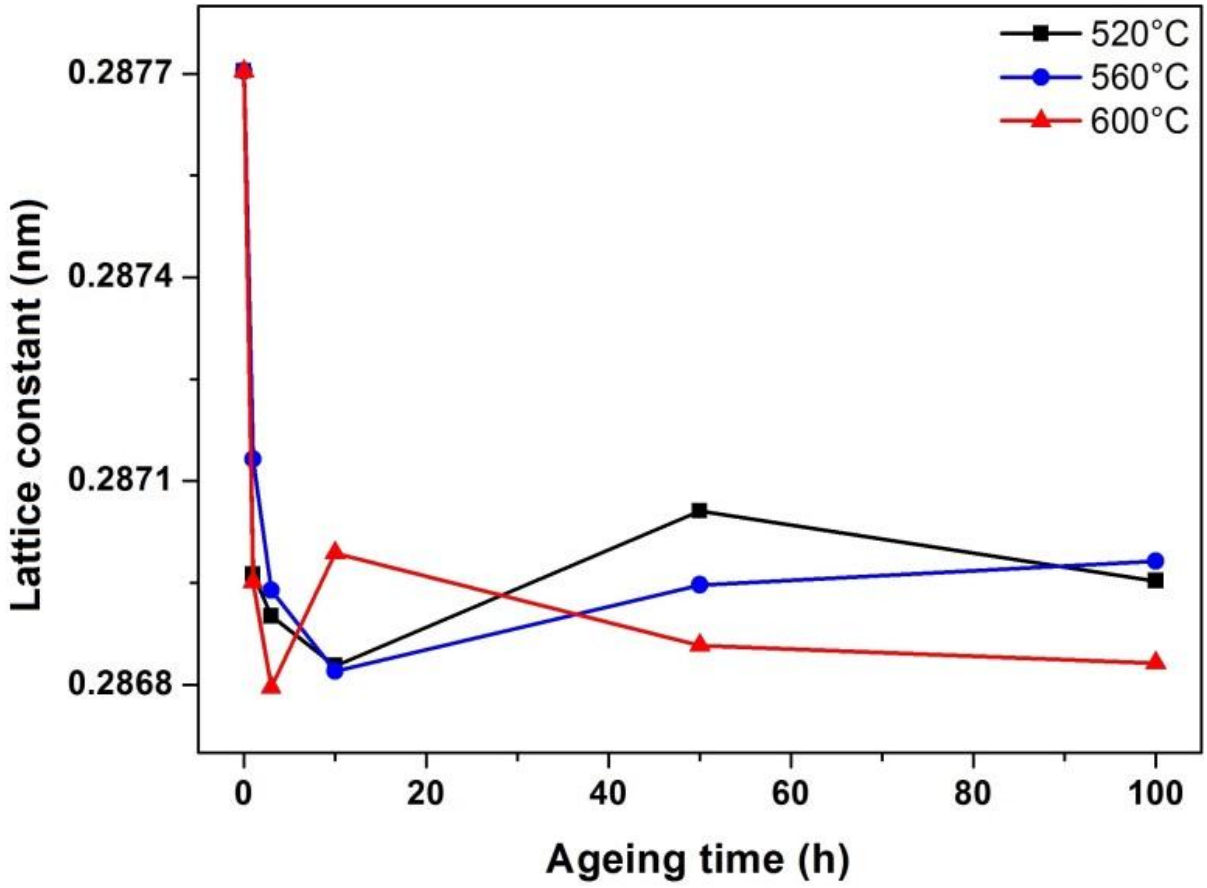

Source: Own author.

5.3.2 Hardness measurements

Figure 5.2 also depicts the Vickers hardness results of both the solution-treated and all aged samples. The material presents a fast increase in hardness values for the first hour of ageing at all temperatures. At high ageing temperature conditions, reverted austenite plays an important role on hardness results of maraging steels. The initial increase in material hardness values indicates that austenite does not exist in these conditions, and precipitate formation should be

responsible for this hardness gain. For the first hour of ageing, the higher the temperature, the higher the hardness value. Possibly the volume fraction of the precipitate formed at this ageing time increases when ageing temperature rises. After 3 h of ageing a similar behaviour is seen at hardness curves of the 520 and 560°C ageing temperature, and a continuous decrease is noted. Similar results were found at an earlier study [19] about this same material aged at 510°C. For the samples aged at 600°C, this decrease starts after 1 h of ageing. This is in accordance with what was discussed in the previous section about the volume fraction of reverted austenite. However a comment must be made regarding the sample aged at 560°C for 3 h. Although austenite has been detected in this condition, its hardness value continues to rise. One possible explanation for this is that the estimated value of austenite in this case was around 1.2%, while for samples aged at 520°C for 10 h and at 600°C for 3 h, the calculated values were 4.6 and 6.1% respectively. The extremely low volume fraction of reverted austenite found in this condition may possibly be smaller than the volume fraction of the precipitates already formed and therefore still does not influence the hardness results of the material.

The hardness values found at the early stages of ageing at this paper are similar to that found in the same material when aged at 480°C (due to the formation of A_3B precipitate types). Sha et al. [19] also suggest that Ni_3Ti-type precipitates form first on Maraging-300 steel aged at 510°C. This suggests that formation of A_3B-types precipitates should be responsible for hardness improvement of the material at the early stages of ageing at high temperatures.

5.3.3 Mössbauer analysis

Figure 5.4 shows the Mössbauer spectra of the solution-treated (ST) sample. A hyperfine field distribution evidencing the ferromagnetic martensitic matrix was used for best fitting. The isomer shift (δ) and quadrupole splitting (2ε) of martensite are close to zero. The former is expected for a Fe^0 metallic alloy, and the latter demonstrates that the tetragonal distortion of the martensitic matrix is minimal in this case and this phase can be considered as bcc. The spectrum possesses a broad linewidth suggesting the existence of a great number of environments and also that the solute atoms are randomly distributed around the Fe atoms.

Figure 5.4 -Mössbauer spectrum of Maraging-300 steel solution-treated at 820°C for 30 min.

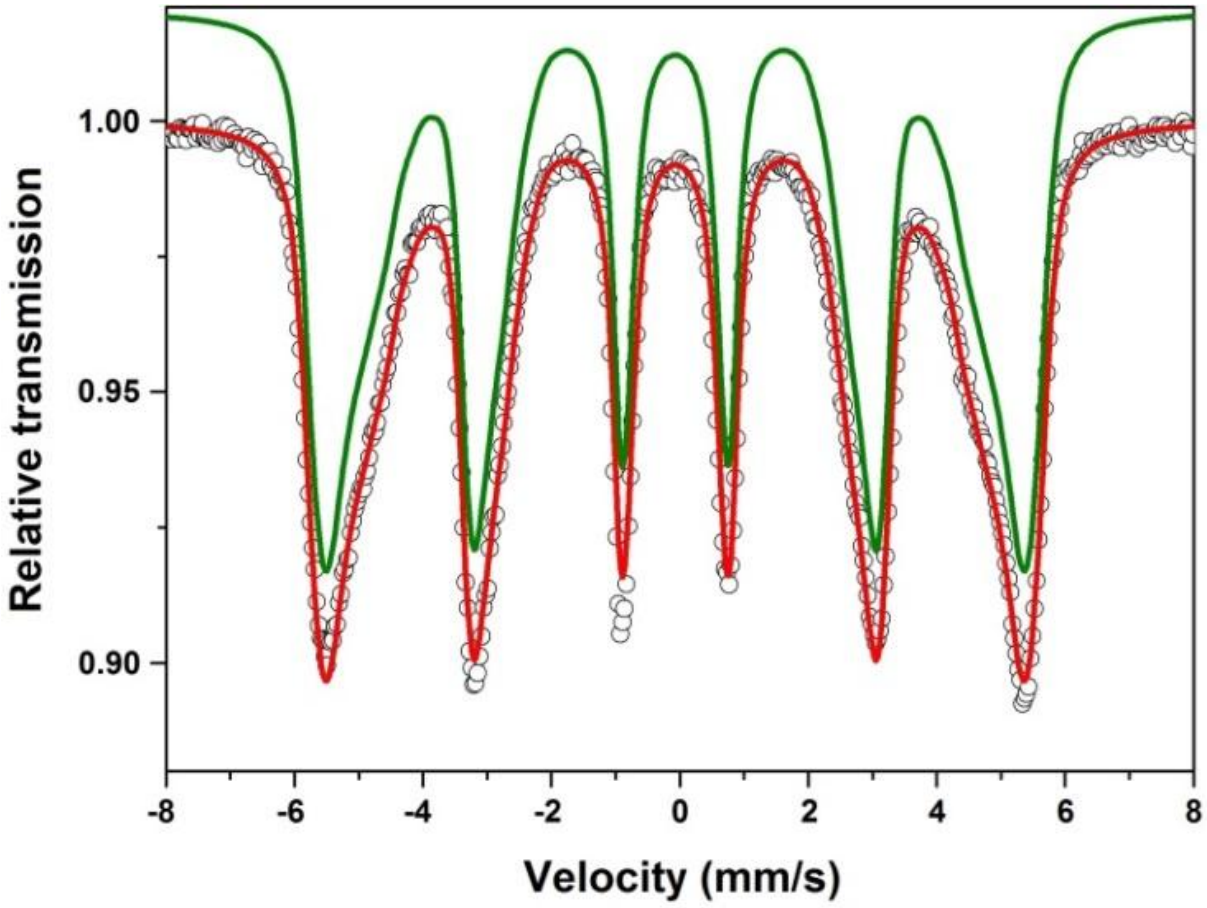

Source: Own author.

The Mössbauer spectra of all the samples aged at various conditions are shown in Figure 5.5. A hyperfine field distribution and a singlet were used for best fitting in all cases. The distribution belongs to the martensitic ferromagnetic phase. The same isomer shift (δ) and quadrupole splitting (2ε) behaviour of the ST sample is observed in these samples but a narrower linewidth was detected, suggesting a decrease in the number of environments around the Fe sites. For higher temperatures and longer times, the appearance of straight line regions on the top of spectrum between the main spectral lines is clear. This is related to the appearance of low magnetic hyperfine field regions that will be discussed later. The paramagnetic contribution increases from 1 h of ageing and suggests that there is a paramagnetic phase (or phases) containing a fraction of Fe in these specimens. Since austenite was not detected at initial ageing times, this paramagnetic peak is likely due to the precipitation of intermetallic compounds that contain some Fe. For higher ageing times and longer temperatures most of the paramagnetic contribution may be attributed to the reverted austenite, but the existence of superimposed singlets

cannot be excluded, thus the coexistence of precipitates and reverted austenite is possible at these conditions. When reverted austenite begins to form, it becomes very hard to state how much of the paramagnetic contribution in the sample is due to the presence of the austenite itself or the paramagnetic precipitates.

In this study, two distribution models were used for the best fit of the spectra, depending on the ageing time and temperature. The first model with magnetic hyperfine fields between 23 and 39 T was used for most of the samples and the second model with B_{hf} from 7.5 to 39 T for samples with longer ageing times and higher temperatures. This was due to the difficulty of adjusting these last samples using the first model, indicating that there were some regions of the material with extremely low magnetic hyperfine fields. In this paper, the analysis was carried out taking into account two parts of the distribution, the high hyperfine field region (23 to 39 T) and the low hyperfine field region (7.5 to 23 T).

Figure 5.5 -Mössbauer spectra of Maraging-300 steel solution-treated at 820°C for 30 min and aged at various conditions.

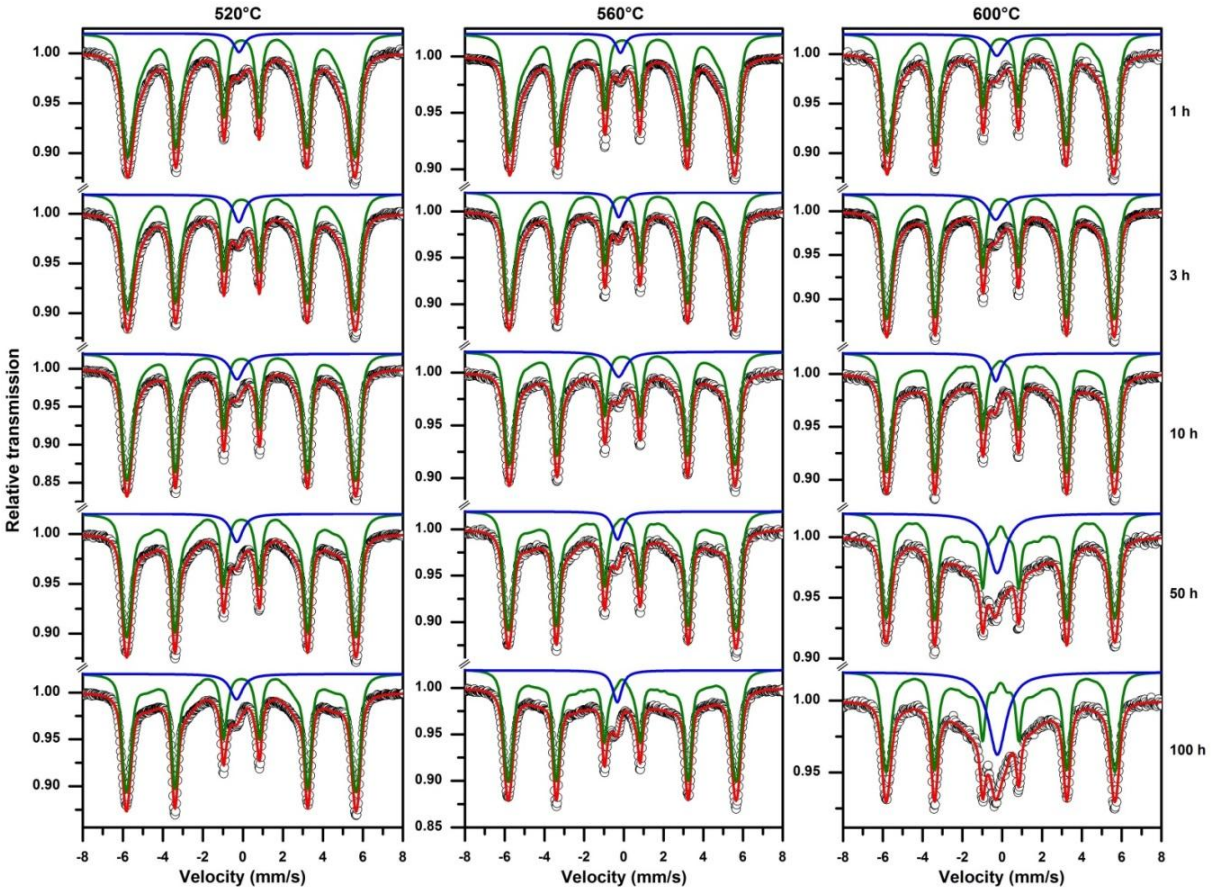

Source: Own author.

The probability distribution curves of the high hyperfine field region for all samples are shown in Figure 5.6. The graphics show a notable change at all the hyperfine field regions in the initial stages of ageing, confirming an intense atomic rearrangement mainly at the first hour. After ageing for 1 h the hyperfine field region changes slow down, indicating that the atomic redistribution is still in progress, but more slowly. This indicates that the composition of the martensitic matrix is becoming constant as ageing proceeds and that much of the atomic redistribution occurs between the intermetallic compounds and the austenitic phase at these conditions.

Figure 5.6 -Probability distribution curves of the high hyperfine field region of Maraging-300 steel solution-treated and aged at various conditions.

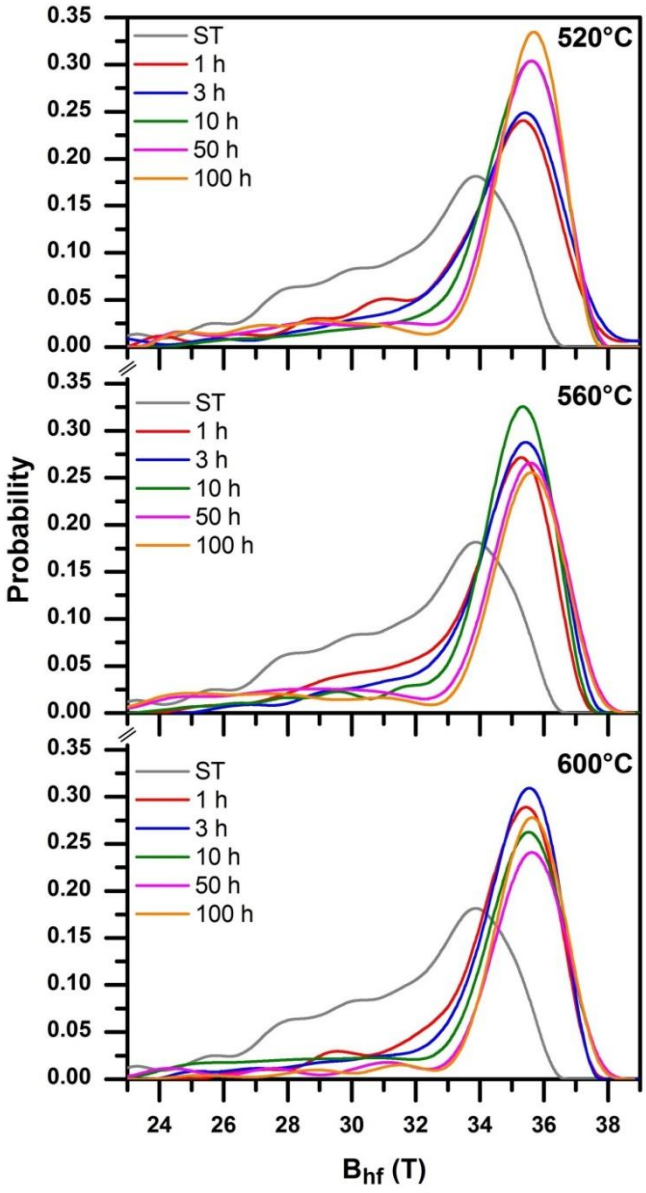

Source: Own author.

At all ageing temperatures, the highest peak suddenly moves towards the high hyperfine field region at the first hour of ageing. This suggests that at this initial stage high amounts of alloying elements leave the martensitic matrix, probably to form precipitates with or without Fe atoms. Mo and Ti are probably the main elements that are responsible for this behaviour since they present a negative contribution to the magnetic hyperfine field of a ^{57}Fe nucleus. This is also in accordance with the results discussed in previous sections and presented in Figure 5.3. This trend is continuous until 100 h of ageing at all temperatures, but it slows down after 1 h of ageing. At the same time, there is an increase at the probability of the highest peak while there is a decrease at the probability of the lower hyperfine field region (23 $<B_{hf}<$ 32 T). This demonstrates that more and more Fe atoms are surrounded by elements that present a positive contribution to the magnetic hyperfine field of a ^{57}Fe nucleus as ageing proceeds. There is an abrupt change at the probability curve between the samples aged for 3 and 10 h at 520°C. This is probably due to the formation of reverted austenite between these two stages. For the samples aged at 560 and 600°C the probability of the highest peak decreases at longer ageing times. This is due to the formation of the low magnetic hyperfine field regions (7.5 $<B_{hf}<$ 23 T) on these samples, besides the remarkable increase at the amount of Fe atoms in the paramagnetic regions of the samples.

The probability distribution curves of the low hyperfine field region at their respective samples are shown in Figure 5.7. Three phenomena can be cited to explain the low hyperfine field region. The first would be the increase in temperature, a fact that can be disregarded since the measurements were performed at RT. The second alternative would be the appearance of phases with high concentration of elements that have a negative contribution to the magnetic hyperfine field of a ^{57}Fe nucleus, in our case Mo and/or Ti atoms. This could explain the appearance of the peak around 21 T, but it does not justify the peaks around 10 and 14 T, since for this the concentration of these alloying elements around the Fe site would have to be extremely high. By considering a statistical distribution for the alloying elements in the martensitic lattice and estimating some representative values for the B_{hf} at the iron site, it is easy to understand that such a concentration of these alloying elements is very unlikely to happen, even for the peak around 21 T. The best explanation for this phenomenon in some samples would be a region of the material that is in

transformation between the ferromagnetic phase and the paramagnetic phases. In this case most probably between martensite and austenite since the latter has a high volume fraction under certain conditions. In these regions there must be a volume of material still not completely transformed in austenite, presenting a transition between the crystalline structures bcc and fcc, thus a magnetic hyperfine field with very low values still exists. Since this phenomenon was detected for the samples aged at 560°C for 50 h and at 600°C for 10 h but not for the specimen aged at 520°C for 100 h, it is reasonable to think that the volume fraction of the reverted austenite may be the responsible for it, and it starts when the austenite fraction is between 29 and 30% (see Figure 5.2). Since the phase transition (α'→γ) causes some distortion in the matrix, probably the volume fraction cited above is the limit from which the distortion of the lattice becomes large enough to hold some regions of the material in an intermediate crystalline structure, demonstrating that the reversion of austenite has not been completed for these ageing conditions. Nunes et al. [9] found similar results when studying Maraging-350 through Mössbauer spectroscopy. The increase at the probability of very low magnetic hyperfine fields as ageing proceeds suggests the migration of Fe atoms from the ferromagnetic to the paramagnetic phases.

Figure 5.7 -Probability distribution curves of the low hyperfine field region of Maraging-300 steel solution-treated and aged at some high temperature/time conditions.

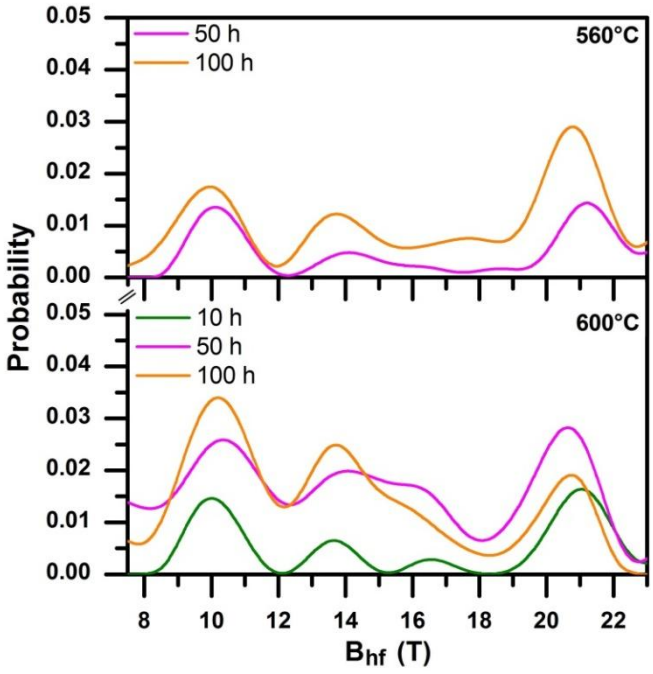

Source: Own author.

An analysis of the two fitting models was performed and showed a competition between the fractional area of the singlet and that of the very low hyperfine field (< 12 T). This analysis indicates that the fractional area of the singlet can be added to the fractional area of the distribution for very low hyperfine fields, and this result can be considered as representative of the amount of Fe that is in a paramagnetic environment in the sample. The fractional area of the low hyperfine field distribution between 12 and 23 T can be considered as the amount of Fe that is in the environment in transformation from the ferromagnetic to the paramagnetic phases. A representation of this can be seen in Figure 5.8.

Figure 5.8 - Fe fraction of the paramagnetic contribution (black bars) and of the very low (red bars) and low (blue bars) hyperfine field regions.

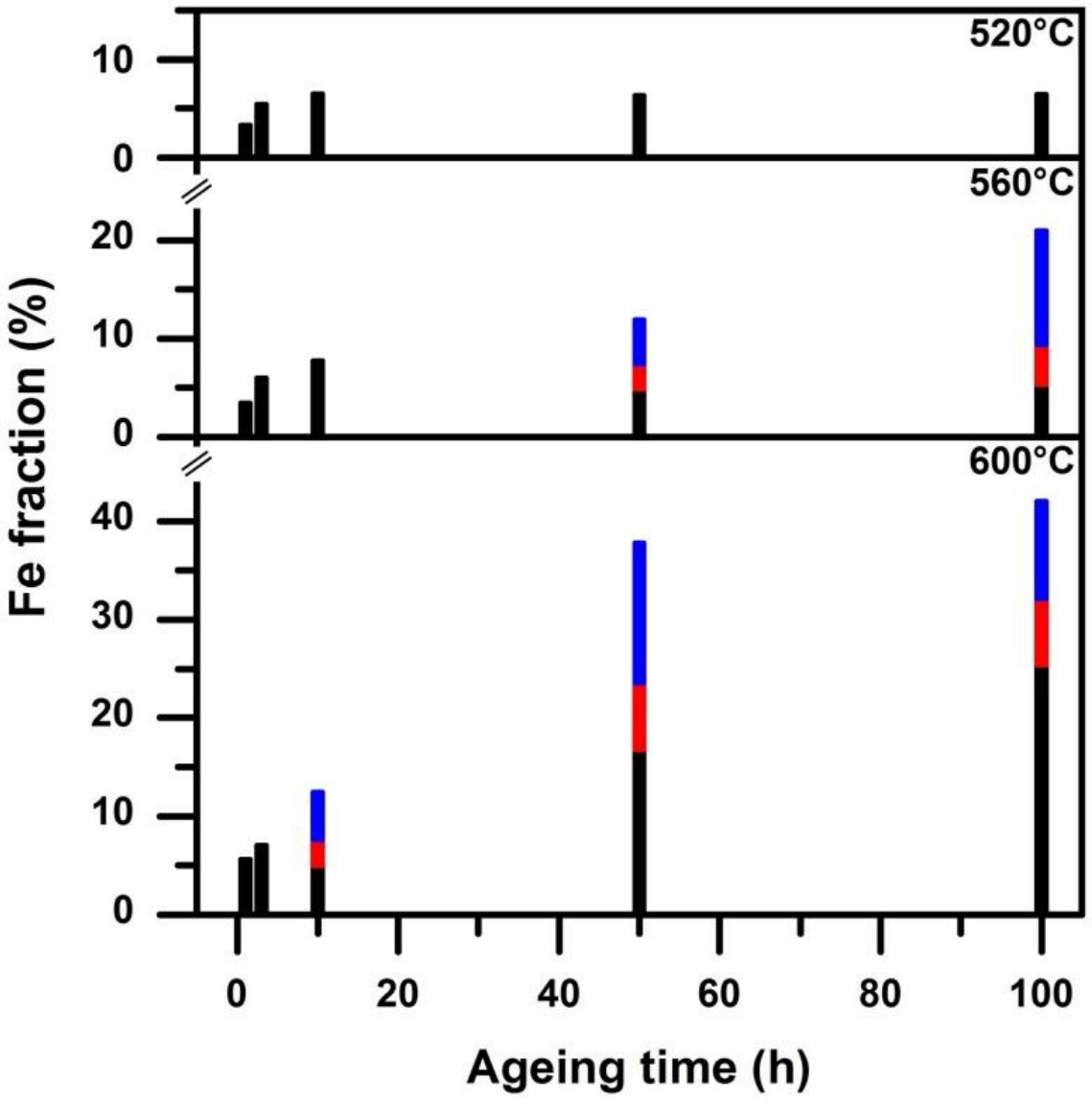

Source: Own author.

For the samples aged at 520°C, the paramagnetic phase(s) account for about 3% of the total Fe in the specimen aged for 1 h, a value that increases to about 6% after ageing for 10 h, probably due to the formation of reverted austenite, and remains constant until 100 h. Sha et al. [19] also reported an increase in Fe content of the austenitic phase of Maraging-300 steel when aged at similar conditions at 510°C between 4 and 8 h. At higher ageing temperatures the phase transformation zones occur, and the total amount of iron that is in a paramagnetic or in a transition environment increases progressively. This is a very realistic result since the longer the ageing time and the higher the temperature, the greater the amount of the Ni-Fe-rich reverted austenite phase formed. Nunes et al. [9] reported that the equilibrium state is reached for Maraging-350 when aged at 650°C for 12 h. The proportional reduction of the fractional area of the low and very low hyperfine fields (7.5 to 23 T) relative to the fractional area of the paramagnetic regions represented in the graph for the sample aged at 600°C for 100 h indicates a tendency for this to occurs for Maraging-300 steel. So for longer times and/or higher ageing temperatures the transition region in the material must not exist anymore, and the two major bcc and fcc phases will exist in a higher degree of coherency, in addition to possible precipitates. This result is in agreement with the meta-equilibrium trend of the sample indicated by the hardness and austenite fraction curves shown in Figure 5.2. Probably at higher ageing temperatures in the material under study the reversion of austenite will be completed. More research at temperatures above 600°C has to be made to evidence this.

5.3.4. Transmission electron microscopy (TEM)

TEM was performed on the specimen aged for 10 h at 560°C. Figure 5.9(a) shows the selected area diffraction pattern (SADP) of the sample and its corresponding bright-field (Figure 5.9(b)) and complementary dark-field images (Figures 5.9(c) and (d)). Figure 5.9(a) shows the diffracted spots used for imaging (spots 1 and 2). Figure 5.9(b) shows the characteristic bright-field image, showing the matrix with dispersed phases. In Figure 5.9(c), using diffraction from spot 1, large plates of reverted austenite are seen, and Figure 5.9(d) (diffraction from spot 2) shows the precipitates at this ageing condition. Finely dispersed spherical precipitates with maximum size of about 35 nm and smaller amounts of needle-like precipitates with dimensions of the order of 10 × 25 nm were found. In maraging

steels, intermetallic compounds present some inter-planar spacings that are closely matching each other [20]. The measured inter-planar spacing of the spots in addition to shape and size analysis suggest that both A_3B and Mo-rich types (probably Fe_7Mo_6) of precipitate are present at this condition. These results are in accordance with what was studied by Li and Yin [5] in a similar maraging steel, which reported the existence of plate-like austenite and suggested the reaction $Ni_3(Ti,Mo) \rightarrow Fe_2Mo + \gamma$(Ni-rich) when ageing at high temperatures. Sha et al. [19] also show the presence of rod-shaped Ni_3Ti and spheroidal Fe_7Mo_6 precipitates when the ageing time is not very long. This compilation of results confirms the coexistence of reverted austenite and at least two types of intermetallic compounds and reveals that the paramagnetic contribution of this condition (see Figure 5.5) is actually a representation of at least three superimposed singlets. This kind of overlapping probably occurs in most of the conditions studied in this paper.

Figure 5.9 -(a) SADP obtained from Maraging-300 steel aged at 560°C for 10 h showing diffraction spots from austenite and precipitates; (b) bright-field TEM image; (c) dark-field image from spot 1 showing large plates of austenite; (d) dark-field image from spot 2 showing precipitates.

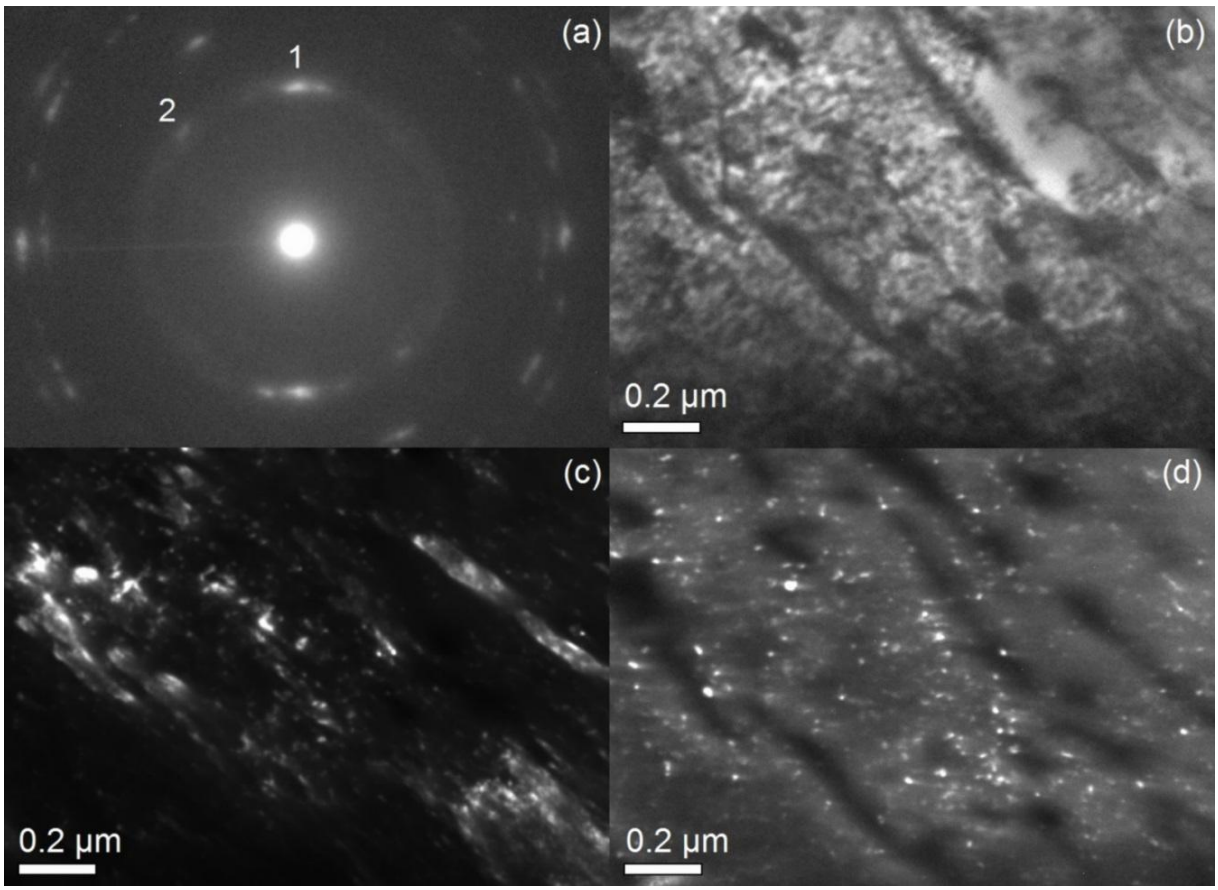

Source: Own author.

5.4. Conclusions

Compiling the results shows that at any temperature studied, atomic redistribution is intense in the first hour of ageing. The paramagnetic phases occur in the material in all aged conditions studied, from the early stages of ageing (intermetallic compounds) to the longest ageing times (austenite + precipitates). At least two different types of precipitates were detected in the material. The Fe content of the martensitic matrix decreases with ageing time, and as soon as austenite begins to form much of the atomic redistribution occurs between this phase and the precipitates. A crystalline/magnetic transition zone was detected in the material for longer times and higher ageing temperatures.

REFERENCES

[1] ASM Specialty Handbook: Nickel, Cobalt, and Their Alloys, ASM International, 2000.

[2] R. Tewari, S. Mazumder, I.S. Batra, G.K. Dey, S. Banerjee, Precipitation in 18 wt% Ni Maraging steel of grade 350, Acta Mater. 48 (2000) 1187–1200.

[3] A. Magnée, J.M. Drapier, J. Dumont, D. Coutsouradis, L. Habraken, Cobalt-containing High-strength Steels, Centre d'Information du Cobalt, Brussels, 1974.

[4] J.B. Lecomte, C. Servant and G. Cizeron, A comparison of the structural evolution occurring during anisothermal or isothermal treatments in the case of nickel and manganese type Maraging alloys, J. Mater. Sci. 20 (1985) 3339–3352.

[5] X.D. Li and Z.D. Yin, Reverted austenite during aging in 18Ni(350) Maraging steel, Mater. Lett.24 (1995).239–242.

[6] V.K. Vasudevan, S.J. Kim, C.M. Wayman, Precipitation reactions and strengthening behavior in 18 wtpct nickel Maraging steels, Metall. Trans. A 21 (1990) 2655–2668.

[7] J.M. Pardal, S.S.M. Tavares, M.P. Cindra Fonseca, H.F.G. Abreu, J.J.M. Silva, Study of the austenite quantification by X-ray diffraction in the 18Ni-Co-Mo-Ti Maraging 300 steel, J. Mater. Sci. 41 (2006) 2301–2307.

[8] J.M. Pardal, S.S.M. Tavares, M.P. Cindra Fonseca, M.R. da Silva, J.M. Neto, H.F.G. Abreu, Influence of temperature and aging time on hardness and magnetic properties of the Maraging steel grade 300, J. Mater. Sci. 42 (2007) 2276–2281.

[9] G.C.S. Nunes, P.W.C. Sarvezuk, T.J.B. Alves, V. Biondo, F.F. Ivashita, A. Paesano Jr., Maraging-350 steel: Following the aging through diffractometric, magnetic and hyperfine analysis, J. Magn. Magn.Mater. 421 (2017) 457–461.

[10] X.D. Li, Z.D. Yin, H.B. Li, T.C. Lei, M.L. Liu, X.W. Liu, M.Z. Jin, Mössbauer study of the early stages of aging in 18Ni (350) Maraging steel, Mater. Chem. Phys. 33 (1993) 277–280.

[11] N. Bouzid, C. Servant, O. Lyon, Anomalous small-angle X-ray scattering from a Maraging alloy during martensiteunmixing, Phil. Mag. B 57 (1988) 343–359.

[12] C. Servant, N. Bouzid, A comparative analysis of the precipitation phenomena occurring in Ni and MnMaraging alloys using small-angle neutron scattering experiments, Phil. Mag. B 60 (1989) 659–687.

[13] Y. Okada, J. Endo, T. Nakayama, Identification of the precipitates in Maraging steels by non-aqueous electrolyte extraction method, Tetsu-to Hagané 69 (1983) 703–710.

[14] K.D. Moore, P.L. Jones, H.F. Cocks, A positron annihilation study of the precipitation hardening effects in a Maraging steel, Phys. Status Solidi (a) 72 (1982) K223–K227.

[15] Z.D. Yin, X.D. Li, M.Z. Zheng, M.L. Liu, X.W. Liu, M.Z. Jin, Mössbauer study of the early stages of ageing in an Fe-19Co-14Mo-10Ni Maraging steel, J. Mater. Sci. Lett. 12 (1993) 179–181.

[16] X.D. Li, Z.D. Yin, Mössbauer study of the aging behavior of 18Ni(350) Maraging steel, Mater. Lett. 24 (1995) 235–238.

[17] X. Li, Z. Yin, H. Li, Mössbauer study of the 430°C decomposition of 18Ni(350) Maraging steel, J. Mater. Sci. Lett. 15 (1996) 314–316.

[18] B.D. Cullity, Elements of X-ray diffraction, second ed., Addison-Wesley, Reading, MA, 1978.

[19] W. Sha, A. Cerezo, G.D.W. Smith, Phase chemistry and precipitation reactions in Maraging steels: Part I. Introduction and study of Co-containing C-300 steel, Metall. Trans. A 24 (1993) 1221–1232.

[20] W. Sha, A. Cerezo, G.D.W. Smith, Phase chemistry and precipitation reactions in Maraging steels: Part IV. Discussion and conclusions, Metall. Trans. A 24 (1993) 1251–1256.

6 CONCLUDING REMARKS

A solution-treated sample and twenty five ageing conditions were studied at this thesis. Appendix-A shows a representation of each ageing condition studied and a table that summarizes what was found at each condition throughout this work.

The sample in the ST condition presented a martensitic matrix without evidence of formation of precipitates or other phases. Its TMS result presents a broad linewidth when compared to that of the aged samples. This indicates a great number of different environments around the Fe atom. However, it cannot be stated that the solution treatment at the conditions performed in this work reached its goal of homogeneously distributing the alloying elements atoms in the matrix. The progressive narrowing of the linewidth of the ferromagnetic matrix at all investigated temperatures shows that the number of different environment surrounding the Fe atoms decreases with increasing ageing time. It becomes evident that the matrix composition reaches its equilibrium the longer the ageing time.

Through TMS analyses it was possible to verify the existence of paramagnetic phases representing the formation of precipitates in almost all of the studied conditions. Through the TEM analyses it was possible to visualize the formation of precipitates in four of the studied conditions (6, 8, 10 and 18). In two of them (10 and 18) the coexistence of precipitates and reverted austenite was also evidenced. A comment must be made about some of the ageing conditions. No precipitates were found by TMS at the conditions 1, 3 and 5. This shows that there are no Fe-content precipitates at these conditions, but the possibility of existing precipitates without iron cannot be completely ruled out. In any case more detailed studies, specifically in these conditions must be carried out to verify this. In condition 6, no precipitates were found in the TMS analysis; however precipitation of intermetallic compounds was detected by TEM. This reinforces what was said about the samples aged at 440°C.

A statement can be made for all the aged samples cited above. Due to the absence of a paramagnetic contribution at the TMS analysis of these samples, some

of the most known phases in maraging steels, such as Laves and μ phases, in addition to any others containing iron, certainly do not exist at these conditions.

It was not possible to state which types of precipitates exist in each of the conditions, but it was possible to confirm and/or discard their formation in some conditions. The atomic redistribution shown through the probability distribution curves and through the variation of the lattice parameters gave us some interesting new information about the rearrangement of the solute atoms in and out of the matrix. In general the atomic redistribution is more intense in the first hours of ageing at temperatures from 480°C.At 440°C the redistribution occurs in as lower and progressive way and the formation of metastable phases was suggested.

Due to its high negative contribution to the hyperfine magnetic field at the ^{57}Fe nucleus, the Mo atom (see Table 6.1) becomes the main responsible for the existence of the low hyperfine field region of these distributions. The decrease in the probability of these regions in the aged samples beyond the displacement of the higher peak to the right shows that Ti and specially Mo atoms are the most likely types of atoms to form precipitates, even with lower concentrations when compared to Ni and Co atoms. At some conditions this suggests that unknown precipitates must be forming. Furthermore, because the size of these atoms is much larger than the Fe, Ni and Co atoms, the output of these alloying elements from the matrix to form precipitates could also be confirmed by the decrease of the lattice parameter of the martensitic matrix.

Another interesting result is the crystalline/magnetic transition zone discussed in chapter 4. More research at ageing temperatures above 600°C has to be made to better investigate this. Also, in situ experiments at these temperatures must be made to clarify this transition phenomenon.

Finally, this study shows us that the combination of Mössbauer spectroscopy with other techniques provides a reliable and effective set of tools to investigate Fe-based alloying steels.

6.1 Suggestion for future work

There are a number of open issues that still need to be addressed in order to provide a clear precipitate kinetics understanding on maraging steels. On the next section, a project in progress and its preliminary results and the difficulties associated to it is presented.

6.1.1 A solution to the quantification problem of precipitated phases in maraging steel

According to the studies of Cook [1],Ni et al. [2] and Ni et al. [3], the development of a theoretical model based on random distribution of non-iron atoms is a powerful tool to investigate the phase transformation process of Fe-based alloying steels. The classic studies of Vincze and Campbell [4] and Wertheim and Jaccarino [5] brought up basic important information regarding the effect of different non-iron solute atoms on the magnetic hyperfine field of a ^{57}Fe nucleus in Fe-based alloys.

Although at this thesis Mössbauer spectroscopy was used as the main technique to provided important information about the atomic mobility in maraging steel, the analysis provided only qualitative results. In maraging steels, the precipitates size is one of the biggest problems that make them hard to analyse. Even when these precipitates are identified, the quantification of their volumetric fraction is neither easy nor trivial. In maraging steels, some few studies [6,7] approaching this topic were done. At these studies the approach is commonly made based on some assumptions about the type and volume fraction of precipitate formed. In addition, the formation of reverted austenite becomes a considerable problem at higher temperatures and longer ageing times.

With the aim of providing a tool capable of help in solving the quantification problem of precipitated phases in maraging steel, some modelling algorithms have been developed by the author of this thesis and a group of partner researchers.

The first studies [4,5] about the contribution of impurity elements on the magnetic hyperfine field of a ^{57}Fe nucleus found out that the values of the contributions for the elements positioned to the left of iron in the periodic table of

elements are negative, while the opposite occurred to the elements positioned to the right. In maraging steels, when analysing the four main alloying elements, two of them have a positive contribution (Ni and Co) and the other two have a negative contribution (Mo and Ti). According to Ovchinnikov [8], in the solution of specific problems, we can confine ourselves to considering the interaction only with the nearest and next-nearest neighbours of the resonant nuclei. Also, the contributions from the nearest and next-nearest neighbours of the iron atom are additive. The values of these contributions for the main alloying elements of maraging steels at the first two coordination spheres are shown in table 6.1.

Table 6.1 - Contributions per near neighbor atom to the magnetic hyperfine field of a ^{57}Fe nucleus.

Element	**Change of magnetic field (T) per atom [4]**	
	$\Delta\langle B_{hf}\rangle_1$	**$\Delta\langle B_{hf}\rangle_2$**
Fe	0.0	0.0
Ni	0.94	0.7
Co	1.33	0.6
Mo	-3.87	-3.16
Ti	-1.91	-1.91

Source: Adapted from Vincze and Campbell [4]

Still according to Ovchinnikov [8], the effective magnetic hyperfine field B_{hf} of the iron atoms, which do not have any atoms of the impurity in their nearest and next-nearest neighbours, has a tendency to increase in comparison with $\langle B_{hf}\rangle_\alpha$ in pure iron. According to Wertheim and Jaccarino [5], the following relationship can be used to calculate the effective magnetic hyperfine field:

$$B_{hf} = \langle B_{hf}\rangle_\alpha (1 + kc)(1 + h_1 n + h_2 m) \quad (6.1)$$

Where $\langle B_{hf}\rangle_\alpha$ is the field in pure iron, $h_1=\Delta\langle B_{hf}\rangle_1/\langle B_{hf}\rangle_\alpha$ and $h_2= \Delta \langle B_{hf}\rangle_2/\langle B_{hf}\rangle_\alpha$ with n nearest and m next-nearest impurity atoms, c is the atomic concentration of impurity atoms and the multiplier(1+kc) is a field amplification factor. A comment must be made regarding the k factor. This factor is calculated empirically for each type of material and takes into account the contribution of impurity atoms of the remote coordination spheres. The k factor is related to the nature of the impurity atoms and is proportional to the concentration of these impurities. Its value is always

positive for any type of impurity atom considered. Some examples of k values can be seen in the study of Wertheim and Jaccarino [5]. At this study, the k factor was computed for binary alloys and a maximum value of about 0.06 was found for Fe-Sn alloys. This factor is easy to calculate for binary Fe-X alloys or even for alloys that have only negative or positive contributions impurity atoms. The work of Cook [1] deduced the value of 0.76 as the k factor for a stainless steel with 34%at. of alloying elements. The calculus of this factor could only be realized due to some considerations that were made in that work. Anyway, the calculus of the k factor is a problem for the present work. A decision about considering or not the k factor on modelling and how to calculate this factor for maraging steel are problems that have to be solved.

Because of the uncertainties about the best way to calculate the results, three algorithm models have been developed. The differences between them are the used value of the contribution to the magnetic hyperfine field of a ^{57}Fe nucleus, besides the fact of considering the contribution of groups of impurity atoms or of each atom separately. In the grade of maraging steel studied at this work, Ni, Co, Mo and Ti are the main alloying elements. These alloying elements account for almost 99% of the impurity atoms of the steel. Other elements like Al, Mn, Si, Cr, Cu, V and C are present, but only in residual fractions. Besides this, a final decision still has to be made about considering or not these (or some of these) alloying elements on calculus.

The first two models (called M1 and M2) have been developed considering two groups of atoms. A positive effect (Ni group) from Ni and Co atoms, accounting for almost 86% of the impurity atoms and a negative effect (Mo group) from Mo and Ti, accounting for more than 12% of the impurity atoms. For the first model (M1), Ni and Mo were considered as major elements in their respective groups and only the values of their contributions (see table 6.1) to the magnetic hyperfine field were taken into account on the calculus of the probability and magnetic hyperfine field functions. This model was based on the study of Ni et al. [3]. Due to the higher relative proportion between the impurity atoms of the present study when compared to the latter study, for the second model (M2) a composed mean considering the contributions of the four main alloying elements and their respective concentration

was made. At this case the values used were $\langle B_{hf}\rangle_{1\text{-}Ni}$ = 1.07 T, $\langle B_{hf}\rangle_{2\text{-}Ni}$ = 0.67 T, $\langle B_{hf}\rangle_{1\text{-}Mo}$ = -3.40 T and $\langle B_{hf}\rangle_{2\text{-}Mo}$ = -2.86 T. For the third model (M3) a more detailed attempt has been developed, considering the specific contributions of each type of impurity atom in the alloy.

In a bcc structure, an iron atom has 8 nearest-neighbors and 6 next-nearest neighbors. Considering a random distribution of solute atoms and following Ni et al [3], an equation was developed to compute the probability $P(Ni_1,Mo_1,Ni_2,Mo_2)$ of an iron atom having Ni_1 and Mo_1 atoms of Ni and Mo respectively in the nearest-neighbor positions and Ni_2 and Mo_2 atoms of Ni and Mo respectively in the next nearest-neighbor positions in a bcc martensitic phase. This equation has been used on models M1 and M2.

$$P(Ni_1, Mo_1, Ni_2, Mo_2) = C_{Ni_1}^{8} c_1^{Ni_1}(1-c_1)^{8-Ni_1} \quad (6.2)$$
$$\times C_{Ni_2}^{6} c_1^{Ni_2}(1-c_1)^{6-Ni_2}$$
$$\times C_{Mo_1}^{8-Ni_1}\left(\frac{c_2}{1-c_1}\right)^{Mo_1}\left(1-\frac{c_2}{1-c_1}\right)^{8-Ni_1-Mo_1}$$
$$\times C_{Mo_2}^{6-Ni_2}\left(\frac{c_2}{1-c_1}\right)^{Mo_2}\left(1-\frac{c_2}{1-c_1}\right)^{6-Ni_2-Mo_2}$$

Where C is a binomial coefficient shown in equation 6.3 and c_1 and c_2 are the atomic concentrations of Ni and Mo group atoms in Maraging-300 steel respectively.

$$C_b^a = \frac{a!}{b!(a-b)!} \quad (6.3)$$

In the study of Ni et al. [3], an equation similar to the equation 6.4 was used to calculate the corresponding magnetic hyperfine field $B_{hf}(Ni_1,Mo_1,Ni_2,Mo_2)$ of an iron atom having all possible configurations of the impurity atoms at the nearest-neighbor and the next nearest-neighbor positions:

$$B_{hf}(Ni_1, Mo_1, Ni_2, Mo_2) = \quad (6.4)$$
$$\langle B_{hf}\rangle_\alpha + Ni_1 \times \Delta\langle B_{hf}\rangle_{1-Ni} + Mo_1 \times \Delta\langle B_{hf}\rangle_{1-Mo}$$
$$+Ni_2 \times \Delta\langle B_{hf}\rangle_{2-Ni} + Mo_2 \times \Delta\langle B_{hf}\rangle_{2-Mo}$$

But at that work the author does not say the reference for this equation. One has to note that this equation does not take into account de field amplification factor (1+kc) and the author even does not explain something about it. We can conclude that the author has completely disregarded this factor, thus inserting a possible error on its calculations. The decision about using or not the field amplification factor for this work reflects in what equation (6.1 or 6.4) will be used to construct the model.

For the third model (M3), a more detailed equation to compute the probability $P(Ni_1,Co_1,Mo_1,Ti_1,Ni_2,Co_2,Mo_2,Ti_2)$ had to be used, since at this model we are considering each of the impurity atoms separately.

$$P(Ni_1,Co_1,Mo_1,Ti_1,Ni_2,Co_2,Mo_2,Ti_2) = C_{Ni_1}^{8} c_1^{Ni_1}(1-c_1)^{8-Ni_1} \quad (6.5)$$

$$\times C_{Ni_2}^{6} c_1^{Ni_2}(1-c_1)^{6-Ni_2}$$

$$\times C_{Co_1}^{8-Ni_1}\left(\frac{c_2}{1-c_1}\right)^{Co_1}\left(1-\frac{c_2}{1-c_1}\right)^{8-Ni_1-Co_1}$$

$$\times C_{Co_2}^{6-Ni_2}\left(\frac{c_2}{1-c_1}\right)^{Co_2}\left(1-\frac{c_2}{1-c_1}\right)^{6-Ni_2-Co_2}$$

$$\times C_{Mo_1}^{8-Ni_1-Co_1}\left(\frac{c_3}{1-c_1-c_2}\right)^{Mo_1}\left(1-\frac{c_3}{1-c_1-c_2}\right)^{8-Ni_1-Co_1-Mo_1}$$

$$\times C_{Mo_2}^{6-Ni_2-Co_2}\left(\frac{c_3}{1-c_1-c_2}\right)^{Mo_2}\left(1-\frac{c_3}{1-c_1-c_2}\right)^{6-Ni_2-Co_2-Mo_2}$$

$$\times C_{Ti_1}^{8-Ni_1-Co_1-Mo_1}\left(\frac{c_4}{1-c_1-c_2-c_3}\right)^{Ti_1}\left(1-\frac{c_4}{1-c_1-c_2-c_3}\right)^{8-Ni_1-Co_1-Mo_1-Ti_1}$$

$$\times C_{Ti_2}^{6-Ni_2-Co_2-Mo_2}\left(\frac{c_4}{1-c_1-c_2-c_3}\right)^{Ti_2}\left(1-\frac{c_4}{1-c_1-c_2-c_3}\right)^{6-Ni_2-Co_2-Mo_2-Ti_2}$$

At this equation, c_1, c_2, c_3 and c_4 are the atomic concentrations of Ni, Co, Mo and Ti atoms respectively. Ni_1, Co_1, Mo_1 and Ti_1 are the number of each of the impurity atoms respectively in the nearest-neighbour positions and Ni_2, Co_2, Mo_2 and Ti_2 are the numbers of each of the impurity atoms respectively in the next nearest-neighbour positions.

The same decision has to be taken about which kind of equation (6.1 or 6.6) will be used to calculate the corresponding magnetic hyperfine field

$B_{hf}(Ni_1,Co_1,Mo_1,Ti_1,Ni_2,Co_2,Mo_2,Ti_2)$ of an iron atom having all possible configurations of the impurity atoms at the nearest-neighbour and the next nearest-neighbour positions for model M3.

$$B_{hf}(Ni_1, Co_1, Mo_1, Ti_1, Ni_2, Co_2, Mo_2, Ti_2) = \quad (6.6)$$
$$\langle B_{hf}\rangle_{\alpha} + Ni_1 \times \Delta\langle B_{hf}\rangle_{1-Ni} + Co_1 \times \Delta\langle B_{hf}\rangle_{1-Co}$$
$$+Mo_1 \times \Delta\langle B_{hf}\rangle_{1-Mo} + Ti_1 \times \Delta\langle B_{hf}\rangle_{1-Ti}$$
$$+Ni_2 \times \Delta\langle B_{hf}\rangle_{2-Ni} + Co_2 \times \Delta\langle B_{hf}\rangle_{2-Co}$$
$$+Mo_2 \times \Delta\langle B_{hf}\rangle_{2-Mo} + Ti_2 \times \Delta\langle B_{hf}\rangle_{2-Ti}$$

Where $\langle B_{hf}\rangle_{1\text{-}Ni}$, $\langle B_{hf}\rangle_{1\text{-}Co}$, $\langle B_{hf}\rangle_{1\text{-}Mo}$ and $\langle B_{hf}\rangle_{1\text{-}Ti}$ are the contributions to the magnetic hyperfine field of one Ni, Co, Mo and Ti atom in the nearest-neighbour position respectively. $\Delta\langle B_{hf}\rangle_{2\text{-}Ni}$, $\Delta\langle B_{hf}\rangle_{2\text{-}Co}$, $\langle B_{hf}\rangle_{2\text{-}Mo}$ and $\langle B_{hf}\rangle_{2\text{-}Ti}$ denote the magnetic hyperfine fields of one Ni, Co, Mo and Ti atom in the next nearest-neighbour position respectively.

Once all the possible atomic configurations and their respective probabilities and calculated magnetic hyperfine fields are obtained for each model, it is possible to plot a calculated hyperfine magnetic field distribution curve for each model. At the under construction models of this study, each of the probability/B_{hf} data pair is considered a Gaussian represented by the equation 6.7.

$$G(x) = P \times e^{\frac{-(x-B_{hf})^2}{\sigma^2}} \quad (6.7)$$

Where P is the calculated probability, B_{hf} is the calculated magnetic hyperfine field and σ is an enlargement factor inversely proportional to the field value. The distribution curve is plotted above the summation of all computed Gaussians.

At this point, a comparison can be made between the generated curves and the experimental curves. Since the calculations were based on a random distribution, the experimental data used to be compared with is that of the solution-treated sample. At the current stage of this study, three distribution curves were plotted using the equations 6.2, 6.4, 6.5 and 6.6. The best σ parameters are still been analysed. Still considering the adjustments to be made and all the problems

mentioned above, in general the experimental and calculated curves have quite similar shapes.

However, it was found that the calculated curves are displaced of about 2 T to the right in relation to the curve obtained experimentally. A possible explanation for this is that at the solution-treated condition used at this study, the alloying elements are not perfectly random distributed around the Fe sites. To best conclude something about this, an alternative is to calculate the Warren-Cowley atomic order parameter, as in the study of Whittle and Campbell [9] for Au-Fe alloys. A study of Nunes et al.[10] in a similar maraging steel at the solution-treated condition suggests that the martensitic matrix would be chemically heterogeneous in nanoscale or that iron has different atomic neighbourhoods. Another study of Arabi et al. [11] shows the existence of Ti(N,C) and Ti_2S inclusions at Maraging-300 at the solution-treated condition. The EDX analysis of these particles show that Fe is the main compositional element (wt%.), followed by Ti, C (at the Ti(C,N) types), Ni, Co and around 3.4% of Mo at the TiCN type. Also more than 200 inclusions in one square millimetre were found at this study. Thermochemical calculations suggest that the Ti-X inclusions will be dissolved only at minimum temperatures around 1150°C. In any case, this displacement between the distribution curves is a problem that still needs to be better analysed and understood.

Despite all these details that will still be analysed, some motivating results have been obtained. The main idea of the suggested work is to create an algorithm that is able to predict at least two results. The first is the atomic percentage of alloying elements leaving the martensitic matrix to form precipitates (or paramagnetic phases). This result is expected to be achieved by varying the concentration of the alloying elements in the algorithm used. Thus generating different distribution curves that will resemble the curves obtained experimentally for the aged samples. The second is the atomic configuration of non-iron atoms in the first and second coordination spheres around iron atoms. This information will allow us to know the behaviour of the martensitic matrix while the paramagnetic phases will be forming during the ageing process.

REFERENCES

[1] D.C. Cook, Strain Induced Martensite Formation in Stainless Steel, Metall. Trans. A, vol. 18A, 1987, pp. 201-210.

[2] Z. Ni, X. Wang, J. Wang, E. Wu, Characterization of the phase transformation in a nanostructured surface layer of 304 stainless steel induced by high-energy shot peening, Physica B, vol. 334, 2003, pp. 221-228.

[3] Z. Ni, X. Wang, E. Wu, G. Liu, Martensitic phase transformations in the nanostructured surface layers induced by mechanical attrition treatment, J. Appl. Phys., vol. 98, 2005, 114319 1-6.

[4] I. Vincze, I.A. Campbell, Mössbauer measurements in iron based alloys with transition metals, J. Phys. F: Met. Phys. 3 (1973) 647–663.

[5] G.K. Wertheim, V. Jaccarino, J. H. Wernick, and D. N. E. Buchanan: Phys. Rev. Leg., 1964, vo|. 12, pp. 24-27.

[6] Z. Guo, D. Li and W. Sha, Quantification of precipitate fraction in maraging steels by X-ray diffraction analysis. Mater. Sci. Technol., vol. 20, 2004, pp. 126-130.

[7] Z. Guo, W. Sha and D. Li, Quantification of phase transformation kinetics of 18 wt.% Ni C250 maraging steel, Mater. Sci. Eng. A, vol. 373, 2004, pp. 10-20.

[8] V.V. Ovchinnikov, Mössbauer analysis of the atomic and magnetic structure of alloys, UK, Cambridge International Science Publishing, 2006.

[9] G.L. Whitlte and S.J. Campbell, J. Phys. F, 15 (1985), pp. 693-707.

[10] G.C.S. Nunes, P.W.C. Sarvezuk, V. Biondo, M.C. Blanco, M.V.S. Nunes, A.M. H. Andrade, A. PaesanoJr.,Structural and magnetic characterization of martensitic Maraging-350 steel, J. Alloy. Compd. 646 (2015) pp. 321–325.

[11] H. Arabi, M. Divandari, A. H. M. Hosseini, The effect of Ti contents on the amounts of inclusions formation and mechanical properties of C300 high strength steel. Iranian Journal of Materials Science and Engineering, Vol. 3 (2), 2006, pp 1-8.

APPENDIX A–SUMMARY OF THE CHARACTERISTICS OF EACH AGEING CONDITION

Figure A.1 shows a representation of each aged condition studied at this work.

Figure A.1 – Representation of the 25 different ageing conditions studied at this work.

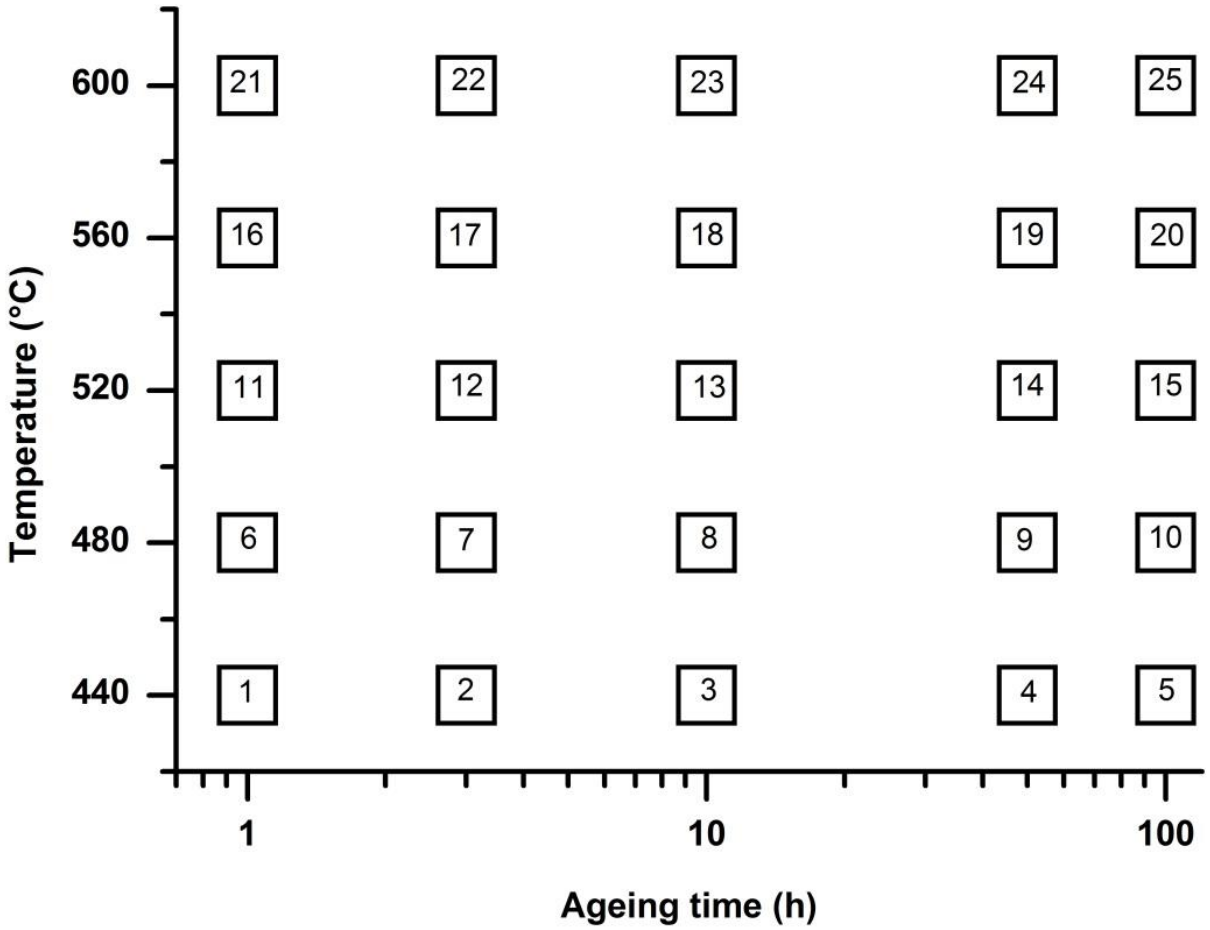

Source: Own author.

With the aim of better understand the phases found at this thesis, table A.1 summarizes what was found at each ageing condition throughout this work. The reverted austenite volume fraction is based on XRD results and the Fe amount values of the paramagnetic phases are based on TMS results. The Fe amount in the brackets takes into account the results found in Chapter 4.

Table A.1 – Summary of the characteristics of each ageing condition.

Ageing condition	Vickers hardness (HV1)	Lattice parameter (nm)	Paramagnetic Phases (%Fe)	Reverted austenite (%)
ST	307±4	0.2877	-	-
1	354±2	0.2871	-	-
2	455±5	0.2872	1.59	-
3	482±7	0.2871	-	-
4	533±1	0.2870	1.31	-
5	618±4	0.2869	-	-
6	533±3	0.2870	-	-
7	575±5	0.2870	3.94	-
8	606±3	0.2869	4.18	-
9	616±2	0.2868	6.45	-
10	592±3	0.2868	5.52	0.92
11	550±6	0.2870	3.33	-
12	585±3	0.2869	5.43	-
13	572±7	0.2868	6.52	3.25
14	518±6	0.2871	6.35	19.05
15	495±3	0.2870	6.47	22.74
16	547±4	0.2871	3.5	-
17	600±2	0.2869	6.06	0.64
18	552±2	0.2868	7.79	10.24
19	563±1	0.2870	4.91 (7.42)	27.4
20	526±2	0.2870	5.32 (9.37)	33.87
21	564±2	0.2870	5.66	-
22	549±1	0.2868	7.09	3.7
23	496±1	0.2870	4.94 (7.63)	24.27
24	469±2	0.2869	16.74 (23.58)	43.8
25	460±1	0.2868	25.39 (32.11)	48.38

Source: Own author.

APPENDIX B– X-RAY POWDER DIFFRACTION PATTERNS

Figure B.1 - XRPD patterns of the as-received (AR) and solution-treated (ST) samples of Maraging-300 steel.

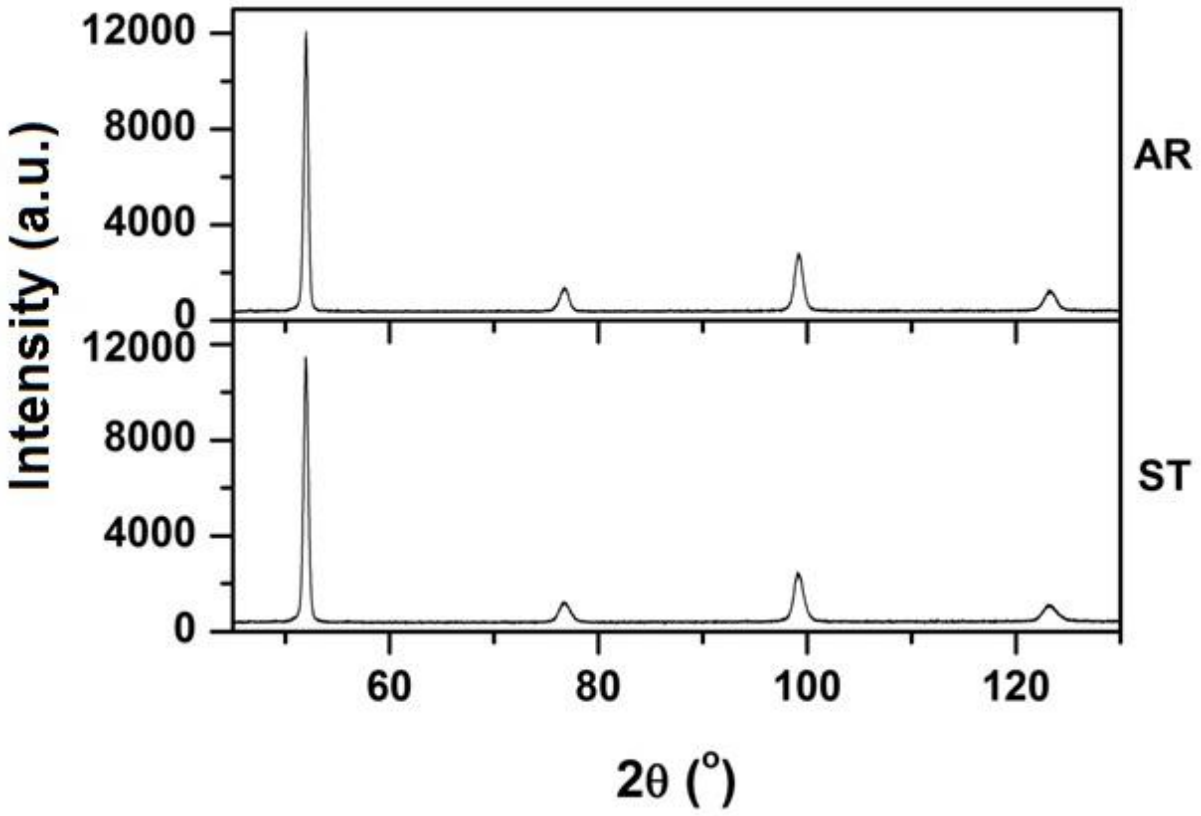

Source: Own author.

Figure B.2 -XRPD patterns of solution-treated and 440°C aged Maraging-300steel specimens.

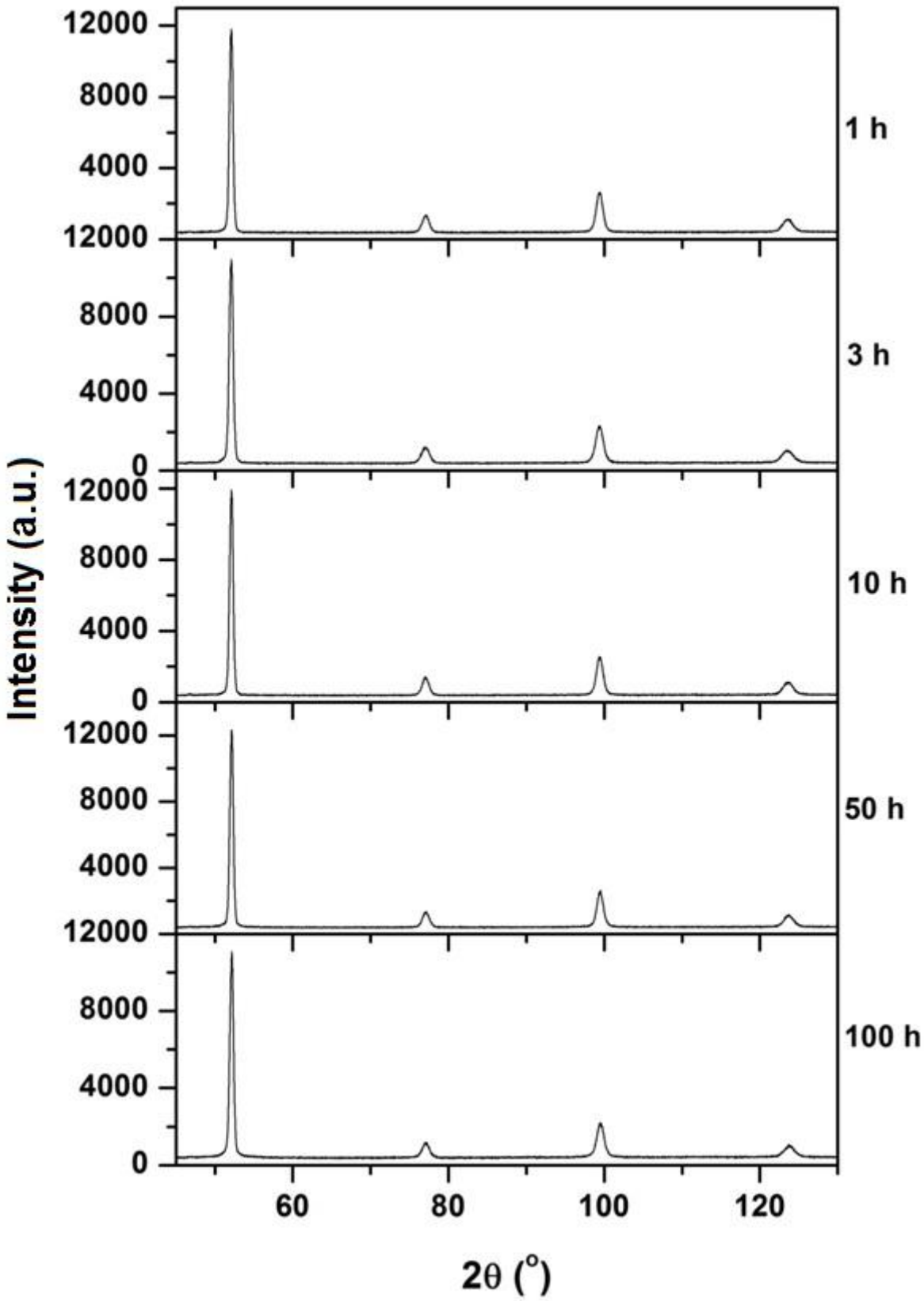

Source: Own author.

Figure B.3 - XRPD patterns of solution-treated and 480°C aged Maraging-300 steel specimens.

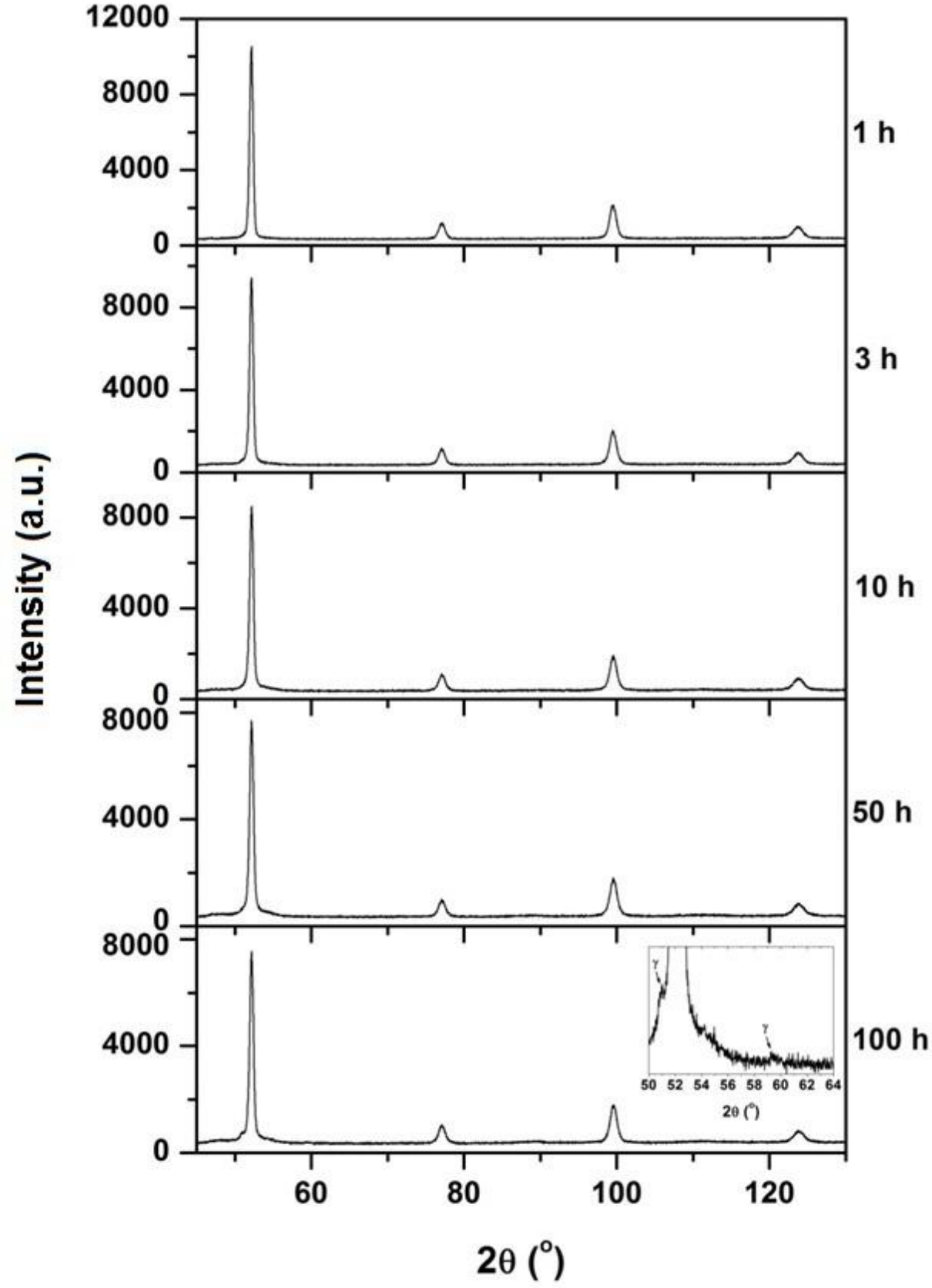

Source: Own author.

Figure B.4 - XRPD patterns of solution-treated and 520°C aged Maraging-300 steel specimens.

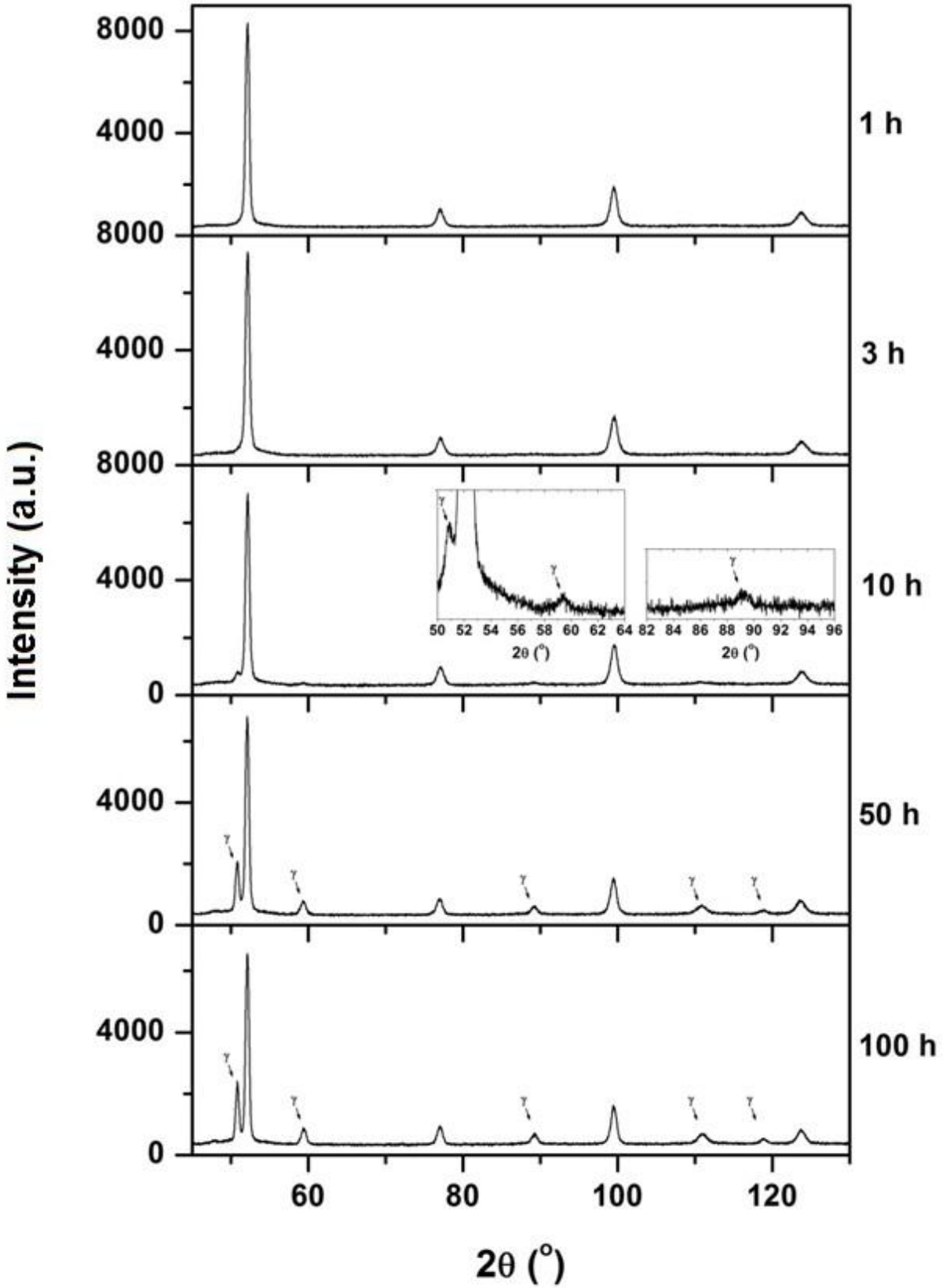

Source: Own author.

Figure B.5 - XRPD patterns of solution-treated and 560°C aged Maraging-300 steel specimens.

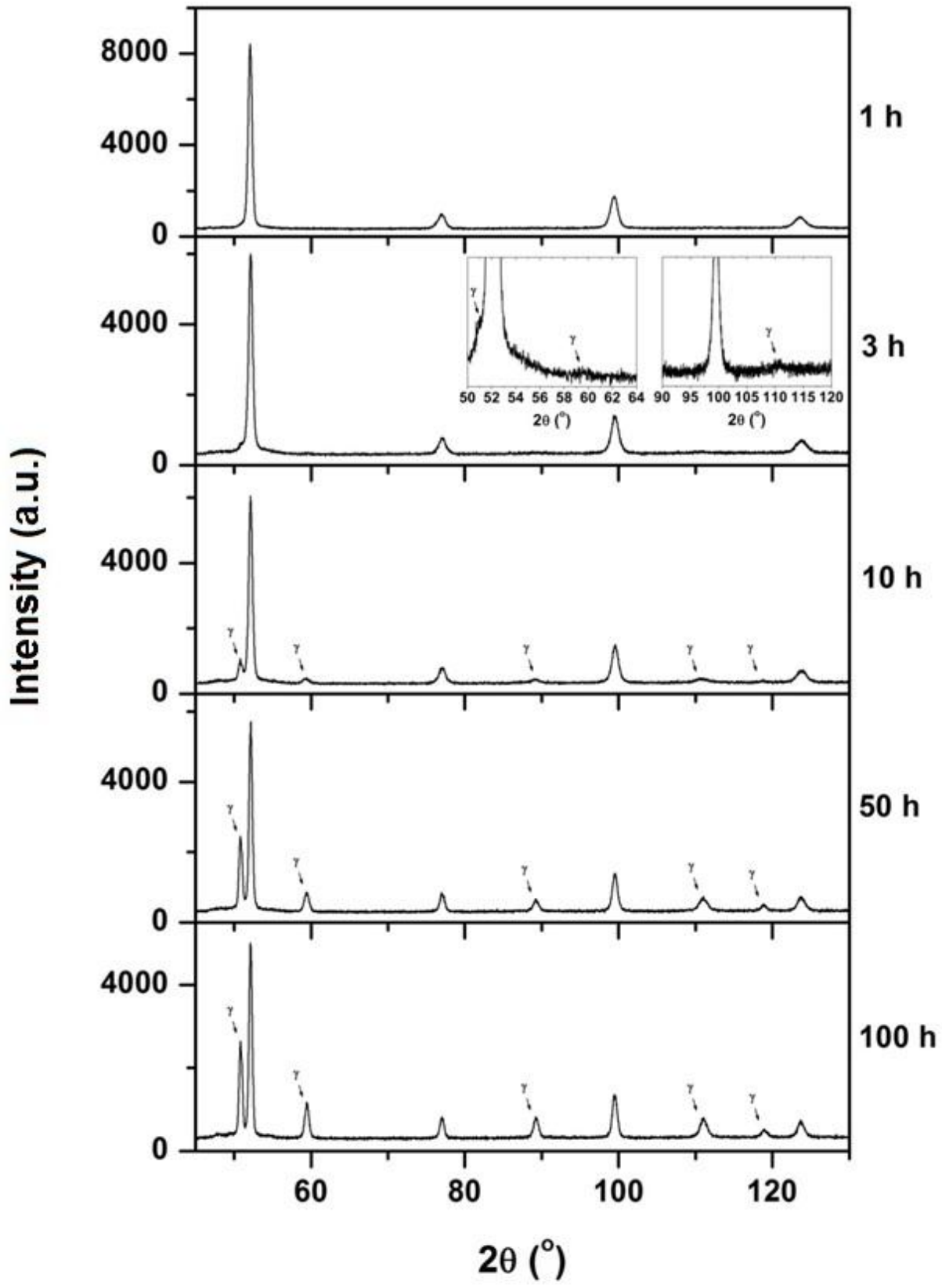

Source: Own author.

Figure B.6 - XRPD patterns of solution-treated and 600°C aged Maraging-300 steel specimens.

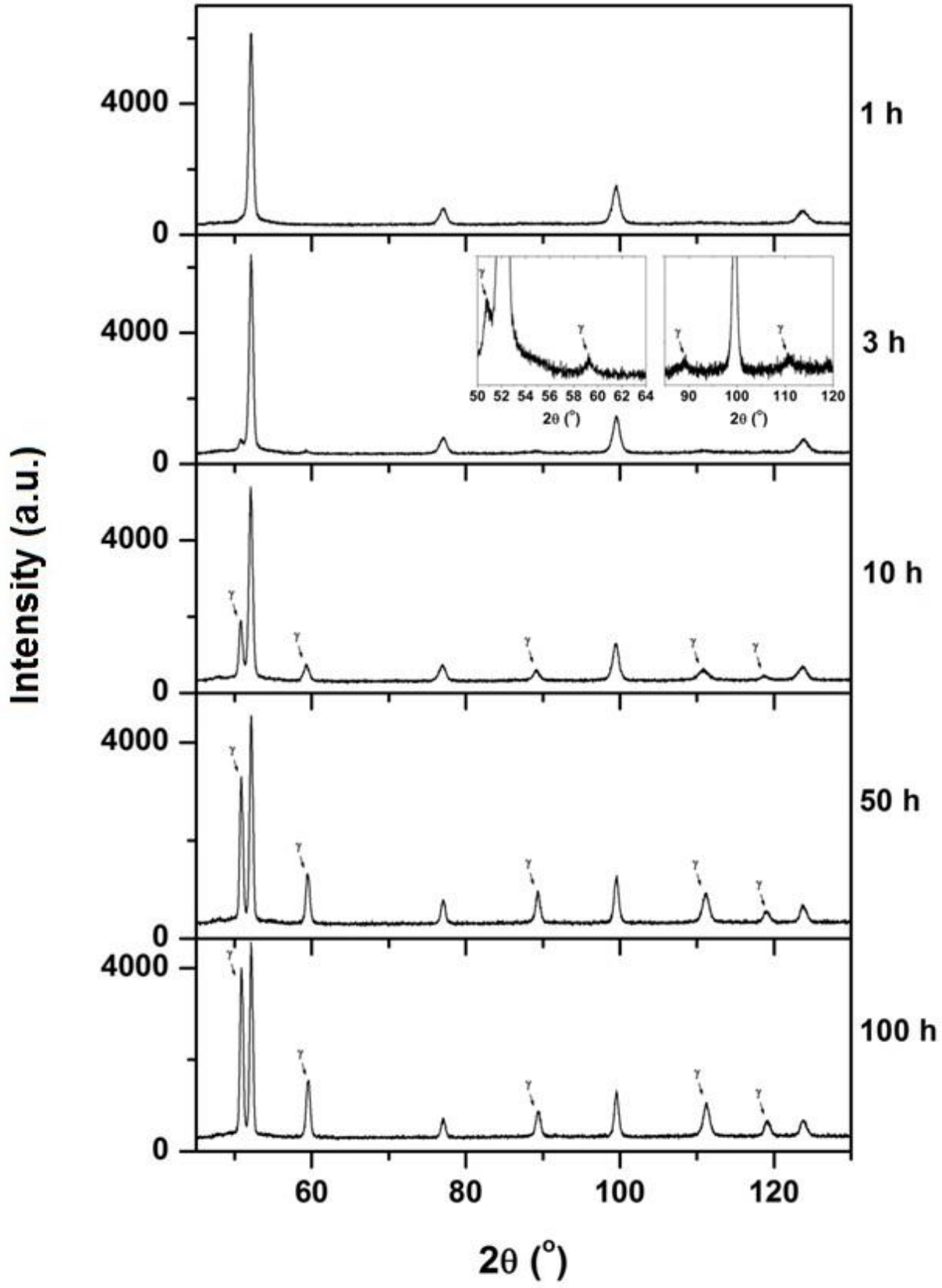

Source: Own author.

APPENDIX C– SCANNING ELECTRON MICROSCOPY OF SOLUTION-TREATED AND 480°C AGED MARAGING-300 STEEL SPECIMEN

A quick SEM study was performed on the specimen that had been aged for 100 h at 480°C and it is shown in figure C.1. The same modified Fry reagent was used. The (reverted) austenitic phase surrounded by the martensitic matrix is evidenced.

Figure C.1 – Reverted austenite surrounded by the martensitic matrix of the solution-treated and 480°C aged specimen.

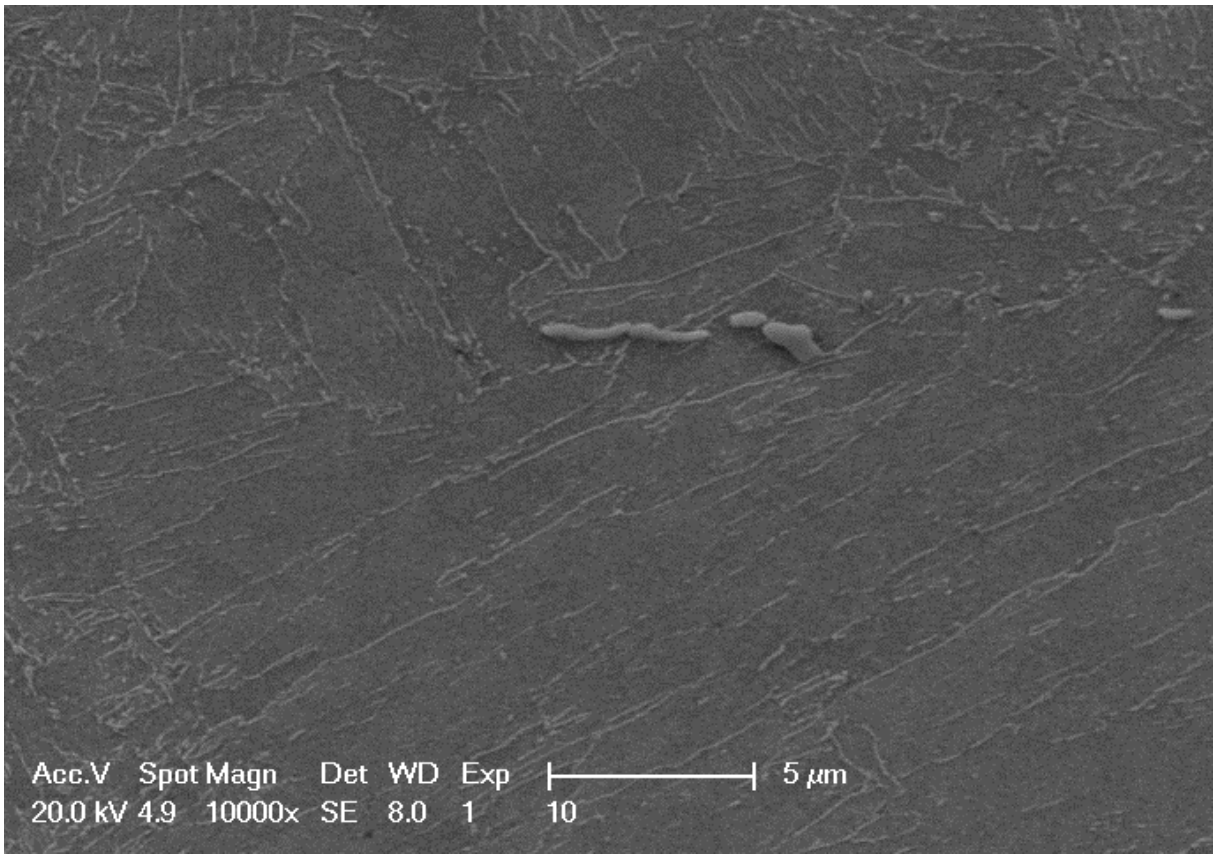

Source: Own author.

APPENDIX D– TRANSMISSION ELECTRON MICROSCOPY MEASUREMENTS

Table D.1 –Measured Interplanar spacings of the TEM analyzed specimens.

Ageing temperature (°C)	Ageing time (h)	Spot	d (nm)
480	1	1	0.2036 (±0.0002)
480	10	2	0.2030 (±0.0012)
480	100	3	0.2076 (±0.0012)
560	10	1	0.2080 (±0.0001)
560	10	2	0.2045 (±0.0005)

Source: Own author.

APPENDIX E– COMPUTATION OF THE MARTENSITIC LATTICE CONSTANT

The lattice constants of the martensitic matrix were computed by plotting the values of a_{hkl} of each diffraction peak of the sample against cos(θ).cot(θ). The a_{hkl} was found by extrapolation. In this example the value of a_{hkl} is 0.287056 nm.

Figure E.1 – Computation of the martensitic lattice constant for the 520°C - 50 h aged condition.

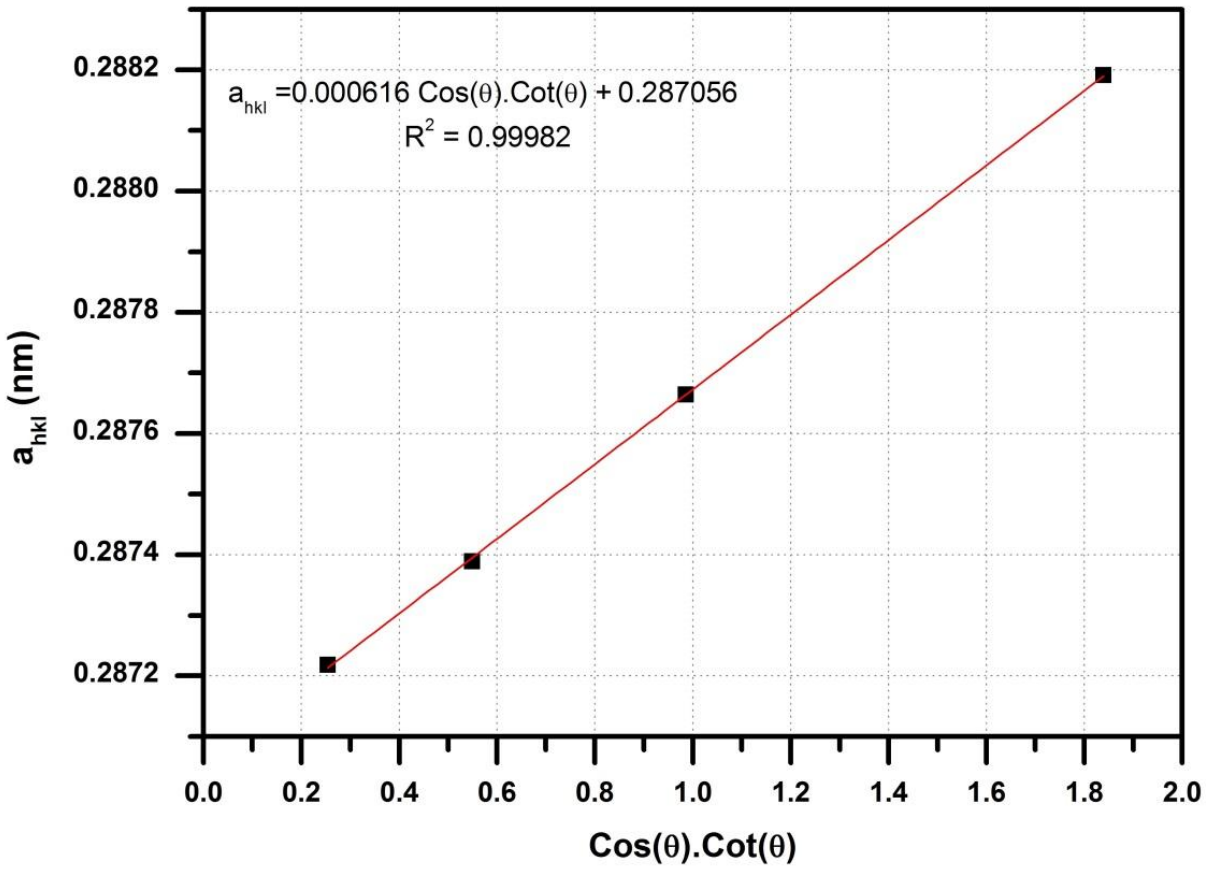

Source: Own author.